MOLECULAR AND CELLULAR BIOLOGY, May 2007, p. 3667–3681 Vol. 27, No. 10
0270-7306/07/$08.00+0 doi:10.1128/MCB.01386-06

Functional Importance of the Anaphase-Promoting Complex–Cdh1-Mediated Degradation of TMAP/CKAP2 in Regulation of Spindle Function and Cytokinesis▽†

Kyung Uk Hong,[1] Young Soo Park,[1] Yeon-Sun Seong,[2] Dongmin Kang,[3] Chang-Dae Bae,[1] and Joobae Park[1]*

Department of Molecular Cell Biology and Samsung Biomedical Research Institute, Sungkyunkwan University School of Medicine, 300 Chunchundong, Jangangu, Suwon, Republic of Korea 440-746[1]; Department of Biochemistry, Dankook University College of Medicine, San 29, Ansuh-dong, Cheonan, Chungnam, Republic of Korea 330-714[2]; and Korea Basic Science Institution, Chuncheon Branch, 192-1 Hyoja 2-dong, Chuncheon, Gangwon-do, Republic of Korea 200-701[3]

Received 28 July 2006/Returned for modification 31 August 2006/Accepted 16 February 2007

Cytoskeleton-associated protein 2 (CKAP2), also known as tumor-associated microtubule-associated protein (TMAP), is a novel microtubule-associated protein that is frequently upregulated in various malignances. However, its cellular functions remain unknown. A previous study has shown that its protein level begins to increase during G_1/S and peaks at G_2/M, after which it decreases abruptly. Ectopic overexpression of TMAP/CKAP2 induced microtubule bundling related to increased microtubule stability. TMAP/CKAP2 overexpression also resulted in cell cycle arrest during mitosis due to a defect in centrosome separation and subsequent formation of a monopolar spindle. We also show that degradation of TMAP/CKAP2 during mitotic exit is mediated by the anaphase-promoting complex bound to Cdh1 and that the KEN box motif near the N terminus is necessary for its destruction. Compared to the wild type, expression of a nondegradable mutant of TMAP/CKAP2 significantly increased the occurrence of spindle defects and cytokinesis failure. These results suggest that TMAP/CKAP2 plays a role in the assembly and maintenance of mitotic spindles, presumably by regulating microtubule dynamics, and its destruction during mitotic exit serves an important role in the completion of cytokinesis and in the maintenance of spindle bipolarity in the next mitosis.

Cytoskeleton-associated protein 2 (CKAP2), also known as tumor-associated microtubule-associated protein (TMAP), LB1, and se20-10, has been identified as a gene that is upregulated in stomach cancers, diffuse B-cell lymphoma, and cutaneous T-cell lymphoma (1, 11, 30). Elevated expression of TMAP/CKAP2 has also been observed in various cancer cell lines (1, 23). However, its cellular functions remain unknown. TMAP/CKAP2 lacks previously identified functional domains and does not share significant homology with other proteins in the current database, which makes it difficult to hypothesize as to its functions. Previous studies have shown that TMAP/CKAP2 mainly localizes to microtubules and centrosomes during interphase and to mitotic spindles during mitosis (1, 23, 30). This observation suggests that the functions of TMAP/CKAP2 might be related to the assembly and/or maintenance of microtubules and mitotic spindles. In support of this idea, a recent study has reported that mouse TMAP/CKAP2 has microtubule-stabilizing properties in NIH 3T3 cells (23).

Microtubules serve a variety of important cellular functions, including intracellular transportation and maintenance of cell shape and cell polarity. At the onset of mitosis, the microtubule network undergoes extensive rearrangements to form a unique bipolar structure, called the mitotic spindle. Multiple factors have been shown to associate with the mitotic spindle and regulate its function by influencing its assembly and dynamics (13, 27). Assembly of a functional bipolar mitotic spindle is critical for faithful segregation of sister chromatids. The centrosome is the main microtubule organizing center in most animal cells (10). Prior to mitosis, the centrosome is duplicated and undergoes a process of maturation. At the G_2-to-M transition, the duplicated centrosomes separate and migrate to opposite sides of the nucleus, priming the assembly of the bipolar mitotic spindle. Thus, centrosome duplication and separation must occur properly to ensure establishment of the bipolar mitotic spindle, segregation of sister chromatids, and maintenance of genomic integrity. Consistent with this notion, abnormalities in centrosome number, size, and morphology have been associated with nearly all human tumor types (33).

Ubiquitin-mediated protein degradation plays an important role in various events during the cell cycle, including mitosis. Anaphase-promoting complex (APC) is an E3 ubiquitin ligase which mediates proteasome-dependent degradation of important mitotic regulators, including securin, mitotic kinases, and cyclins (17). Timely activation of the APC and degradation of its substrates are required for proper progression through mitosis and exit from mitosis. APC is well known for its role in the degradation of securins, which subsequently leads to the loss of cohesion between sister chromatids during the transition from metaphase to anaphase (42, 49). Two WD repeat-containing proteins, Cdc20 and Cdh1, serve as substrate-specific adapters of the APC, thus conferring different substrate specificities. Cdc20 activates the APC during the transition from metaphase

* Corresponding author. Mailing address: Department of Molecular Cell Biology, Sungkyunkwan University School of Medicine, 300 Chunchundong, Jangangu, Suwon, Republic of Korea 440-746. Phone: 82 31 299 6130. Fax: 82 31 299 6149. E-mail: jbpark@med.skku.ac.kr.

† Supplemental material for this article may be found at http://mcb.asm.org/.

▽ Published ahead of print on 5 March 2007.

to anaphase and recognizes substrates containing a destruction box (D box), composed of the sequence RXXL (where X denotes any amino acid), while Cdh1 activates the APC in late mitosis and early G_1 and recognizes substrates containing either a D box or a KEN box (35, 36, 50). Although most studies on the APC have focused on its role in the mitotic spindle checkpoint and in targeting major mitotic regulators for degradation, some studies have suggested that the APC also regulates the mitotic spindle functions during mitosis and reorganization of the microtubule network following mitosis, as proteins that are involved in mitotic spindle functions are among the substrates of the APC (4, 7, 15, 18, 24, 38, 39).

In the present study, we report on the effects of TMAP/CKAP2 overexpression on microtubules and mitotic spindle organization; we also describe the mechanism of TMAP/CKAP2 degradation during mitotic exit and its functional importance. Based on the results of the present study, we propose that TMAP/CKAP2 plays a role in the assembly and maintenance of bipolar spindles by regulating microtubule dynamics, and its destruction during mitotic exit serves an important role in the regulation of the spindle functions and cytokinesis.

MATERIALS AND METHODS

Expression constructs. Generation of an enhanced green fluorescent protein (EGFP) fusion TMAP/CKAP2 construct (pEGFP-C2 CKAP2) has been described previously (1). A myc-tagged TMAP/CKAP2 expression construct (pCMV6-myc-CKAP2, where CMV is cytomegalovirus) was generated by subcloning the PCR-amplified coding sequence of TMAP/CKAP2 into the pCMV6-myc vector (kindly provided by M. J. Hahn, Sungkyunkwan University School of Medicine, Suwon, Republic of Korea). pCAGGS-mCKAP2, an expression construct for mouse TMAP/CKAP2 (mTMAP/CKAP2), was generated by subcloning the PCR-amplified coding sequence of mTMAP/CKAP2 (NM_001004140) into the pCAGGS vector harboring chicken β-actin promoter and a CMV enhancer (kindly provided by H.-W. Lee, Yonsei University, Seoul, Republic of Korea). For generation of myc-tagged Cdh1 and Cdc20 constructs, full-length cDNA clones for human Cdh1/Fzr1 (IMAGE identifier, 3160334) and Cdc20 (IMAGE identifier, 3634656) were purchased from RZPD (Berlin, Germany). The coding sequences were then PCR amplified and subcloned into the pCMV6-myc vector and were subsequently verified by sequencing. The target sequence used for generation of Cdh1 small interfering RNA (siRNA) was 5′-AAUGAG AAGUCUCCCAGUCAG-3′ (9). For a plasmid-based expression of Cdh1, small hairpin loop siRNA (shRNA) and top and bottom templates for the siRNA were designed, annealed together, and subcloned into the pSilencer 2.0-U6 vector (Ambion), according to the manufacturer's instructions. A negative control shRNA expression plasmid was provided by the manufacturer. For generation of the KEN box mutant of TMAP/CKAP2, in which all three residues (amino acids [aa] 80 to 82) were replaced with alanines, and D-box mutants in which arginines were replaced with alanines, a QuikChange II site-directed mutagenesis kit (Stratagene) was used according to the manufacturer's instructions.

Cell culture and transfection. HeLa, HEK 293, and NIH 3T3 cells were cultured in Dulbecco's modified Eagle's medium containing 10% fetal bovine serum and antibiotics and were subcultured every 3 days. For transfection, Lipofectamine Plus (Invitrogen) was used according to the manufacturer's instructions. To control the level of exogenously introduced TMAP/CKAP2 or its mutants, expression constructs were often mixed with an empty vector, usually at a 1:3 ratio for transfection.

Antibodies. Generation and characterization of rabbit polyclonal antiserum to human TMAP/CKAP2 have been previously described (1). For generation of rabbit polyclonal antiserum against mTMAP/CKAP2, glutathione *S*-transferase (GST)–mCKAP2 expressed in bacteria was purified using glutathione-Sepharose beads and eluted by thrombin digestion. Rabbits were then immunized once a week with purified mTMAP/CKAP2 mixed with Freund's adjuvant (Sigma) for 4 to 6 weeks before the antiserum was obtained. The specificity of rabbit polyclonal anti-mTMAP/CKAP2 antibody is shown in Figure S1 in the supplemental material. Mouse monoclonal antibodies against α-tubulin (clone B-5-1-2) and γ-tubulin (clone GTU-88) were purchased from Sigma. Mouse monoclonal antibodies against cyclin B1 (clone GNS1), Plk1 (clone F-8), and Cdc27 (clone AF3.1) and goat polyclonal antibodies against fzr/Cdh1 (N-15), p55 CDC/Cdc20 (N-19), and centrin-2 (N-17) were purchased from Santa Cruz. Mouse monoclonal antibodies against c-*myc* (clone 9E10) and Cdh1 (clone CC43) were purchased from Calbiochem. Mouse monoclonal antibody against Aurora B/AIM-1 (clone 6) was purchased from BD Transduction Laboratories. Rabbit polyclonal anti-APC2 and rat monoclonal horseradish peroxidase (HRP)-conjugated antihemagglutinin (anti-HA) antibodies were purchased from NeoMarkers and Roche, respectively. Cy2-conjugated anti-rabbit immunoglobulin G (IgG) was purchased from Molecular Probes. Cy3-conjugated anti-mouse IgG and Texas Red-conjugated anti-goat IgG were purchased from Rockland.

Degradation assays. Assessment of degradation of endogenous and exogenously introduced TMAP/CKAP2 and its mutants during mitotic exit was done as follows. HeLa cells were transfected with the indicated constructs and, on the following day, were treated with 1 μM nocodazole (Sigma) in complete medium for 16 to 20 h, which resulted in the accumulation of cells at the G_2 or M phase of the cell cycle. Cells that had arrested at prometaphase were collected by gentle pipetting and were either harvested immediately (designated as 0 h) or released from the nocodazole block by two washes in fresh medium; cells were finally released into fresh medium for 2 to 4 h to allow progression through mitosis and exit into G_1. Cells were then either lysed in Laemmli buffer (50 mM Tris-Cl [pH 6.8], 100 mM dithiothreitol, 2% sodium dodecyl sulfate [SDS; wt/vol], 0.1% bromophenol blue, 10% [vol/vol] glycerol) for Western blot analysis or fixed in cold 70% ethanol for fluorescence-activated cell sorting (FACS) analysis. Degradation of TMAP/CKAP2 and its mutants was assessed by Western blot analysis using rabbit polyclonal anti-TMAP/CKAP2 antiserum. The level of α-tubulin served as a loading or internal control. To test the proteasome dependency of degradation, nocodazole-arrested mitotic HeLa cells were collected by gentle pipetting and washed three times in fresh medium (each wash followed by 5 min of centrifugation). After the final wash, cells were resuspended in fresh medium containing either dimethyl sulfoxide (DMSO; vehicle control) or 500 nM epoxomicin (Boston Biochem) and replated onto a dish for 4 h. For degradation assays using ectopic overexpression of Cdh1 or Cdc20, GFP fusion or myc-tagged constructs of wild-type (WT) or various mutants of TMAP/CKAP2 were cotransfected into HeLa cells with a myc vector, myc-Cdh1, or myc-Cdc20 expression plasmid. One day after transfection, cells were harvested for Western blot analysis.

Immunofluorescence staining and image acquisition. Cells grown on glass coverslips were fixed in 3.7% formaldehyde in phosphate-buffered saline (PBS) for 15 min at room temperature and permeabilized in 0.5% Triton X-100 in PBS for 10 min. Following incubation in the blocking solution (5% bovine serum albumin in PBS) for 30 min, the cells were incubated in primary antibody solution (diluted in the blocking solution) for 1 h at room temperature and washed twice in PBS. They were then incubated in a solution of secondary antibodies conjugated to fluorochromes (diluted in the blocking solution) for 1 h at room temperature and washed twice in PBS. They were finally counterstained with DAPI (4′,6′-diamidino-2-phenylindole) and mounted on glass slides using Gel/Mount (Biomeda). Primary antibody dilutions used for the immunofluorescence staining were the following: mTMAP/CKAP2, dilution, 1:200; α-tubulin, 1:5,000; γ-tubulin, 1:100; cyclin B1, 1:100; and centrin-2, 1:150. For centrin-2 staining, cells were fixed in ice-cold methanol instead of formaldehyde. All fluorochrome-conjugated secondary antibodies were used at dilutions of 1:200. Fluorescence images were viewed and acquired using an Axioplan 2 microscope (Carl Zeiss) equipped with an AxioCam charge-coupled device camera (Carl Zeiss). When indicated, an LSM 510 confocal microscope (Carl Zeiss) was used. AxioVision 4.3 software (Carl Zeiss) was used for processing images, and the overlaying and merging of images was done using Adobe Photoshop 7.0 (Adobe).

Western blot analysis. Transfected or treated cells were harvested by boiling samples in 1× Laemmli buffer for 10 min. After the protein concentration was determined by using a bicinchoninic acid protein assay, β-mercaptoethanol was added to each sample, which was then boiled for another 5 min. Protein samples (25 or 50 μg) were resolved by SDS-polyacrylamide gel electrophoresis (PAGE) and transferred to a polyvinylidene difluoride (PVDF) membrane (Millipore). Following 30 min of incubation in the blocking solution (5% skim milk in Tris-buffered saline–Tween) at room temperature, the blot was incubated with an appropriate dilution of the primary antibody (in the blocking solution) for 1 h at room temperature or overnight at 4°C. The blot was washed twice in Tris-buffered saline–Tween and incubated with an appropriate HRP-conjugated secondary antibody (diluted in the blocking solution) for 1 h at room temperature. The antibody-antigen complex was then detected using SuperSignal West Pico solution (Pierce).

FACS analysis. Cells were fixed in cold 75% ethanol overnight or longer. They were spun down, washed in PBS containing 1% bovine serum albumin, and incubated in the propidium iodide (PI) solution containing 50 μg/ml PI, 0.1%

sodium citrate, 0.3% NP-40, 50 μg/ml RNase A, and 1× PBS for 1 h at 37°C. DNA profiles of PI-stained cells were obtained using a FACSCalibur system (Becton Dickinson) and analyzed using CELLQuest software, version 3.3 (Becton Dickinson).

In vivo and in vitro ubiquitylation assays. For the in vivo ubiquitylation assay, HeLa cells were transfected with an HA-tagged ubiquitin expression plasmid (kindly provided by J. K. Shin, Sunkyunkwan University School of Medicine, Suwon, Republic of Korea) alone or cotransfected with a myc-tagged TMAP/CKAP2 expression plasmid. One day after transfection, cells were incubated in 500 nM epoxomicin for 6 h. Cells were collected and lysed in radioimmunoprecipitation assay (RIPA) buffer (20 mM Tris, 100 mM NaCl, 0.5 mM EDTA, 0.5% NP-40, pH 7.5) containing phenylmethylsulfonyl fluoride, aprotinin, and leupeptin. The supernatant was obtained after centrifugation at 10,000 × *g* for 10 min. myc-CKAP2 was then immunoprecipitated by incubating the lysate with mouse monoclonal anti-c-*myc* antibody for 2 h at 4°C, followed by a 1-h incubation with protein G agarose beads (Pierce). Protein G beads were pulled down, washed four times with RIPA buffer, and boiled in 2× Laemmli buffer. Samples were then separated on a 6% SDS-PAGE gel and transferred to a PVDF membrane (Millipore). Polyubiquitylated myc-TMAP/CKAP2 was then detected by immunoblotting with an HRP-conjugated rat monoclonal anti-HA antibody.

For the in vitro ubiquitylation assay, the APC was immunoprecipitated from nocodazole-arrested, mitotic HeLa cell lysates using a monoclonal anti-Cdc27 antibody and protein G-agarose beads as described above. The immunopurified APC was confirmed by immunoblotting for Cdc27 and APC2 (data not shown). Recombinant human Cdh1 was obtained following baculoviral expression of polyhistidine-tagged Cdh1 in High Five (Invitrogen) insect cells. Baculovirally expressed Cdh1 was purified using Ni-nitrilotriacetic acid-agarose beads (QIAGEN) according to the manufacturer's instructions. Human E1 ubiquitin ligase, His_6-UbcH10 (E2), human ubiquitin, ubiquitin aldehyde, and energy regeneration solution were purchased from Boston Biochem. For production of Nus-tagged TMAP/CKAP2 (Nus-CKAP2), the full-length coding sequence of TMAP/CKAP2 was subcloned into pET-44a(+) vector (Novagen). It was introduced to and expressed in an *Escherichia coli* strain BL21 (Novagen) according to the manufacturer's instructions. Expressed Nus-CKAP2 was then purified using Ni-nitrilotriacetic acid agarose (QIAGEN) according to the manufacturer's instructions. Nus-CKAP2 (approximately 80 ng) was incubated with 10 μl of mitotic APC bead suspension in the presence of recombinant Cdh1 and the reagents above in a 20-μl reaction mixture for 1 h at room temperature. For negative controls, mitotic APC beads or Cdh1 was excluded from the reaction. The reaction was stopped by the addition of 5× Laemmli buffer and boiling for 10 min. Samples were then resolved by 6% SDS-PAGE, transferred to a PVDF membrane, and immunoblotted with rabbit polyclonal anti-TMAP/CKAP2 antiserum to detect the presence of high-molecular-weight, polyubiquitylated Nus-TMAP/CKAP2.

Coimmunoprecipitation assay. HeLa cells were cotransfected with GFP-TMAP/CKAP2 and myc-Cdh1 expression constructs. One day after transfection, cells were incubated in 500 nM epoxomicin for 6 h. Cells were collected and lysed in RIPA buffer. After centrifugation at 10,000 × *g* for 10 min, the resulting supernatant was divided and incubated with a monoclonal GST (IgG control), c-*myc*, or GFP antibody for 2 h at 4°C, followed by incubation for 1 h with protein G-agarose beads (Pierce). Protein G beads were then pulled down, washed four times with RIPA buffer, and finally boiled in 2× Laemmli buffer. Samples were then processed for Western blot analysis in the same manner described above using a rabbit polyclonal TMAP/CKAP2 antibody and a monoclonal c-*myc* antibody to detect the presence of coimmunoprecipitated GFP-TMAP/CKAP2 and myc-Cdh1, respectively.

GST pull-down assay. GST, GST-WT, or GST-KENmut TMAP/CKAP2 was expressed in HEK 293T cells by transient transfection and purified using glutathione-Sepharose 4B beads (Amersham Biosciences) according to the manufacturer's instructions. GST fusion protein-bound beads were then incubated with baculovirally purified recombinant His-tagged Cdh1 in the binding buffer (20 mM Tris, pH 7.4, 100 mM NaCl2, 0.5 mM EDTA, 0.5% NP-40) for 2 h at 4°C, followed by four washes in the binding buffer. The bead-bound protein fraction was eluted in 3× Laemmli buffer by boiling for 10 min. The samples were then resolved by 8% SDS-PAGE and immunoblotted using mouse monoclonal antibodies against Cdh1 and GST to detect coprecipitated His-Cdh1 and GST fusion proteins, respectively.

Time-lapse video microscopy. HeLa or HEK 293 cells were transfected on a six-well plate with a GFP-WT or GFP-KEN box mutant TMAP/CKAP2 expression plasmid. Twenty-four hours after transfection, two-channel time-lapse video microscopy was performed using a fully motorized Axiovert 200 M microscope (Carl Zeiss), equipped with Axiocam HRm. Temperature and CO_2 control were maintained using the Incubator S-M and Heating insert M06 controlled by Tempcontrol 37-2 and CTI-Controller 3700. Both bright-field and GFP fluorescence images were acquired for 24 to 48 h with a lapse time of 5 or 10 min using AxioVision 4.3 software. For routine and quantitative analyses, images were acquired using a 20× objective (LD Plan-Neofluar 20×/0.4 Corr Ph2; Carl Zeiss). For quantification of GFP fluorescence intensity, the acquired images were imported into ImageGauge software (Fuji Photo Film). The GFP fluorescence intensity was measured from the area covering an entire mitotic or interphase cell and background fluorescence from a neighboring area was subtracted.

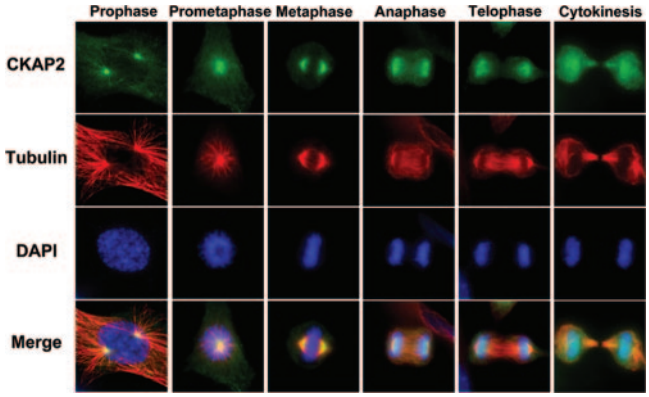

FIG. 1. Subcellular localization of TMAP/CKAP2 during mitosis. NIH 3T3 cells were fixed and doubly immunostained for TMAP/CKAP2 (green) and α-tubulin (red). Representative images of cells at different stages of mitosis are shown.

RESULTS

Subcellular localization of TMAP/CKAP2 during mitosis. Our previous study indicated that expression of TMAP/CKAP2 is cell cycle dependent (22). Both mRNA and protein levels of TMAP/CKAP2 remain low during G_1, start to incline as cells enter S phase, and continue to increase until G_2/M. Such a cell cycle-dependent expression pattern of TMAP/CKAP2 has also been demonstrated by previous microarray studies (21, 47). Previously, we along with others reported that TMAP/CKAP2 mainly localizes to the microtubules as well as to the centrosomes in interphase cells (1, 23, 30, 43). We further characterized the subcellular localization of endogenous TMAP/CKAP2 in NIH 3T3 cells during mitosis when its protein level reaches its maximum. During early phases of mitosis, TMAP/CKAP2 colocalized to the mitotic spindles and spindle poles (Fig. 1), consistent with a previous report (23). However, interestingly, starting at some point during anaphase B, TMAP/CKAP2 was localized near the chromatin region and was no longer associated with spindle or midzone microtubules by telophase. Later, the majority of TMAP/CKAP2 was located at newly formed daughter nuclei, and some of the protein also localized to midbody microtubules within the intercellular bridge (Fig. 1). The pattern of cell cycle-regulated expression and association of TMAP/CKAP2 with mitotic spindles indicated that TMAP/CKAP2 may be involved in the organization and/or regulation of microtubules and mitotic spindles during the G_2/M phases of the cell cycle.

TMAP/CKAP2 overexpression induces microtubule bundling and arrests cells in mitosis. In order to assess the effect of TMAP/CKAP2 on microtubules, HeLa and NIH 3T3 cells were transfected with a GFP or a GFP-fused TMAP/CKAP2

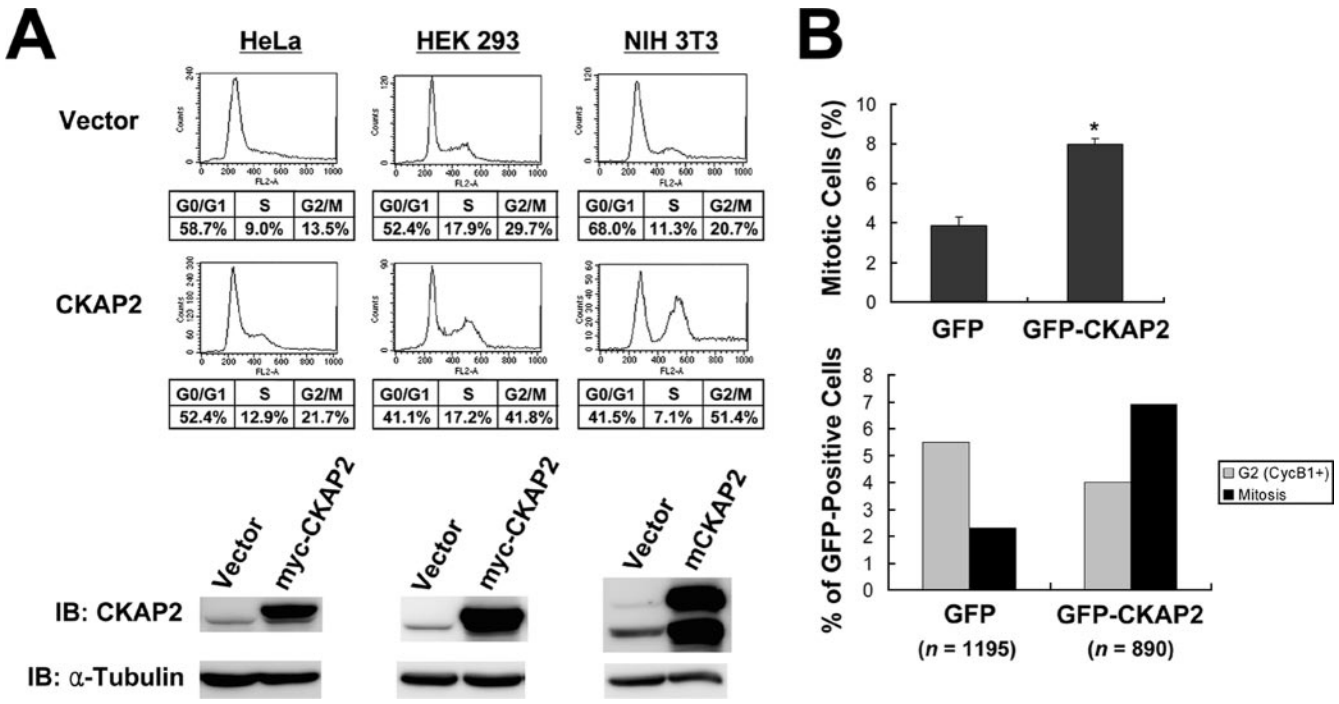

FIG. 2. Overexpression of TMAP/CKAP2 results in mitotic arrest. (A) The proportion of G_2/M cell population is significantly increased in TMAP/CKAP2-overexpressing cells. HeLa or HEK 293 cells were transfected with a vector control (Vector) or a myc-tagged (human) TMAP/CKAP2 expression construct (CKAP2) along with a GFP expression construct. NIH 3T3 cells were transfected with a vector control (Vector) or an mTMAP/CKAP2 expression construct (CKAP2) along with a GFP expression construct. Three days after transfection, transfected cells, i.e., GFP-positive cells, were analyzed by FACS analysis (top). The bottom panels show the level of ectopically introduced TMAP/CKAP2 in each cell type by Western blot analysis. α-Tubulin levels are shown as loading controls. Note that both endogenous and ectopically introduced mTMAP/CKAP2 proteins appear as double bands (see Fig. S1A in the supplemental material). IB, immunoblot. (B) The top panel shows the mitotic index among GFP- or GFP-CKAP2-expressing HEK 293 cells after 2 days of transfection. The bar graphs show the mean values ± standard error of the means from the following calculation: (number of mitotic cells/total number of GFP-positive cells) × 100%. The bottom panel shows the percentage of cytoplasmic cyclin B1-positive (CycB1+) cells at G_2 and the percentage of cells in mitosis among GFP- or GFP-CKAP2-expressing HEK 293 cells after 2 days of transfection. Cells exhibiting cytoplasmic cyclin B1 staining were defined as cells at G_2 phase. *n*, the number of GFP-positive cells analyzed.

(GFP-CKAP2 or GFP-TMAP/CKAP2) construct and examined for any changes in the microtubule network. Interestingly, TMAP/CKAP2 overexpression resulted in microtubule bundling, characterized by formation of thick bundles of microtubules with irregular shapes and curvatures (see Fig. S2A and B in the supplemental material). Moreover, consistent with a previous report (23), microtubules in TMAP/CKAP2-overexpressing cells were more resistant to nocodazole treatment than microtubules in control cells, indicating that TMAP/CKAP2 has microtubule-stabilizing properties (see Fig. S2C in the supplemental material). These results suggested that TMAP/CKAP2 is likely to influence microtubule dynamics during the G_2/M phases of the cell cycle, during which its expression peaks.

To further characterize the effect of TMAP/CKAP2 overexpression and functional outcomes of increased microtubule stability, the cell cycle profile of TMAP/CKAP2-overexpressing cells was examined in various cell types using FACS analysis. HeLa or HEK 293 cells were transfected with an empty vector (control) or a myc-tagged TMAP/CKAP2 expression construct along with a GFP expression construct. NIH 3T3 cells were transfected with a vector control or an mTMAP/CKAP2 expression construct along with a GFP expression vector. At 3 days posttransfection, cells were fixed and PI stained for the FACS analysis. In all of the cell types examined, TMAP/CKAP2 overexpression caused a significant increase in the percentage of cells with 4N DNA content compared to the control cells transfected with the vector alone (Fig. 2A). The effect of TMAP/CKAP2 overexpression on the cell cycle was highly pronounced in NIH 3T3 cells. At 3 days posttransfection, more than half of the cells transfected with TMAP/CKAP2 showed a 4N DNA content (Fig. 2A). These results suggested that the increased number of cells with 4N DNA content following TMAP/CKAP2 overexpression resulted from a significant cell cycle delay or arrest.

Measurement of the mitotic index of TMAP/CKAP2-expressing, GFP-positive cells revealed that TMAP/CKAP2 overexpression resulted in a 2.1-fold increase in the percentage of HEK 293 cells in mitosis (Fig. 2B, top), indicating a cell cycle arrest or delay during the mitotic phase. TMAP/CKAP2 overexpression, however, did not alter the number of cells at G_2, identified by cytoplasmic cyclin B1 immunostaining (Fig. 2B, bottom), suggesting that TMAP/CKAP2 overexpression did not block or cause a significant delay in the progression of G_2 or mitotic entry and that cells at mitotic phase were the most severely affected.

Mitotic spindle defects in TMAP/CKAP2-overexpressing cells. To investigate the nature of the cell cycle delay during

mitosis observed after TMAP/CKAP2 overexpression, cells overexpressing TMAP/CKAP2 were examined by immunocytochemical analysis. HEK 293 and NIH 3T3 cells were utilized for the analysis because the phenomenon of TMAP/CKAP2-induced mitotic arrest was quite pronounced in these cell types (Fig. 2A). HEK 293 cells were transfected with a GFP control or a GFP-CKAP2 construct, and 2 days after transfection, cells were fixed and immunostained for α-tubulin to visualize microtubules. Interestingly, examination of TMAP/CKAP2-transfected cells revealed a large number of mitotic cells with spindle defects. In HEK 293 cells, overexpression of TMAP/CKAP2 induced more than a 9.1-fold increase in the percentage of cells with spindle defects, and these cells constituted approximately 45% of all mitotic cells (Fig. 3A and data not shown).

The most prevalent spindle defect observed in TMAP/CKAP2-overexpressing cells was the formation of monopolar spindles (Fig. 3B), established by elongated microtubules originating from a single centrosomal mass, as identified by immunostaining for γ-tubulin, a centrosome-specific marker (Fig. 3C and D). Additionally, as a result of the abnormal monopolar spindle formation, the condensed chromatids were either arranged in a disorganized manner, failed to align on the metaphase plate, or were pushed to the opposite side of the cytoplasm away from the single spindle pole (Fig. 3C). Relatively high levels of cyclin B1 located along the spindle, as well as the absence of metaphase plates, also indicated that these cells were arrested at a prometaphase-like state and had not yet progressed into anaphase (Fig. 3D). Even the cells with bipolar spindles exhibited abnormal organization of spindle microtubules. TMAP/CKAP2-overexpressing mitotic cells with abnormal bipolar spindles were characterized by the presence of disorganized and elongated spindle microtubules, well-developed interpolar microtubules, and diffuse spindle poles (Fig. 3C). As a result, despite the existence of bipolar spindles, most of these cells failed to possess condensed chromatids aligned in the center of the cell, which suggests that the spindle function is also compromised in these cells. In contrast, among control HEK 293 cells expressing GFP alone, only a few cells were found to have a monopolar spindle or the other spindle defects observed in GFP-TMAP/CKAP2-expressing cells, although cells with multipolar spindles were occasionally observed at a frequency similar to that observed among untransfected cells (Fig. 3B and data not shown), indicating that the spindle defects observed in TMAP/CKAP2-overexpressing cells occurred specifically due to the increased TMAP/CKAP2 protein level. Similar results were also obtained with NIH 3T3 cells (data not shown).

Analysis of GFP-TMAP/CKAP2-expressing HEK 293 cells by time-lapse video microscopy also confirmed that cells expressing relatively high levels of GFP-TMAP/CKAP2 developed monopolar spindles and subsequently arrested at prometaphase, whereas cells expressing relatively low levels of GFP-TMAP/CKAP2 showed normal progression through mitosis (Fig. 4B). After a prolonged period of arrest at mitosis, TMAP/CKAP2-overexpressing cells developing spindle defects failed to complete mitosis normally and underwent one of the following: cell death (11%), exit without cytokinesis (i.e., exiting mitosis without attempting cytokinesis) (24%), asymmetrical division (37%), and cytokinesis failure (i.e., initiating cytokinesis yet failing to complete it) (29%) (Fig. 4A and B). Surprisingly, a relatively large proportion of these cells (66%) eventually attempted to undergo a cell division. However, these cell divisions resulted in either asymmetric distribution of chromosomes and cell material or cytokinesis failure (Fig. 4B, panels b and d). It should be also noted that 53% of the cells with spindle defects formed tetraploid (i.e., 4N) cells by either exiting mitosis without cytokinesis or failing to complete cytokinesis. This suggests that the overall increase in the 4N population induced by TMAP/CKAP2 overexpression (Fig. 2A) can also be attributed to an increase in the number of tetraploid cells in addition to an increase in the number of cells arrested at mitosis.

TMAP/CKAP2 overexpression inhibits centrosome separation. Next, we questioned whether the monopolar spindle formation observed in TMAP/CKAP2-overexpressing cells occurred due to defects in centrosome duplication or in centrosome separation. In order to examine the morphology of centrosomes within these cells, HEK 293 cells were transfected with a GFP-CKAP2 expression construct, and 2 days after transfection, cells were immunostained for γ-tubulin. When observed under low magnification, TMAP/CKAP2-expressing mitotic cells with monopolar spindles appeared to have a single, dense γ-tubulin-immunoreactive spot located at the pole. A closer examination of these single spots often revealed two spots either fused or located close to each other (Fig. 3E), which suggested that duplicated centrosomes might have failed to separate. These observations suggested that TMAP/CKAP2 overexpression may not affect the process of centrosome duplication but, instead, inhibits centrosome separation and/or induces fusion of duplicated centrosomes at the onset of mitosis. This was also supported by the presence of duplicated centrosomes within interphase cells expressing high levels of TMAP/CKAP2 (data not shown). To further confirm this finding, we performed immunostaining of GFP-CKAP2-transfected cells using an antibody against centrin-2, a protein that is localized in the lumen of centrioles (34), to visualize individual centrioles. In contrast to the cells with normal bipolar spindles which had one pair of centrin-2-positive centrioles at each pole, the cells exhibiting monopolar spindles showed the presence of two pairs of centrioles at the pole of the monopolar spindle (Fig. 3E), demonstrating that TMAP/CKAP2-induced monopolar spindle formation, indeed, occurred due to a defect in the process of centrosome separation.

TMAP/CKAP2 is degraded during mitotic exit via the ubiquitin-proteasome pathway. Another interesting observation made during preliminary studies was that the protein level of TMAP/CKAP2 declines abruptly as cells exit mitosis. Based on the observation that an excessive amount of TMAP/CKAP2 protein results in spindle abnormalities (Fig. 3), we postulated that regulation of the TMAP/CKAP2 protein level during the cell cycle has a functional importance, for instance, in regulating microtubule dynamics and/or establishing spindle bipolarity during mitosis. This prompted us to study the mechanism and the functional significance of TMAP/CKAP2 degradation during mitotic exit. First, in order to study the kinetics of changes in the TMAP/CKAP2 protein level during mitotic exit, HeLa cells that were arrested at mitosis by nocodazole treatment were collected and released into fresh medium to allow progression through mitosis. Released cells were then har-

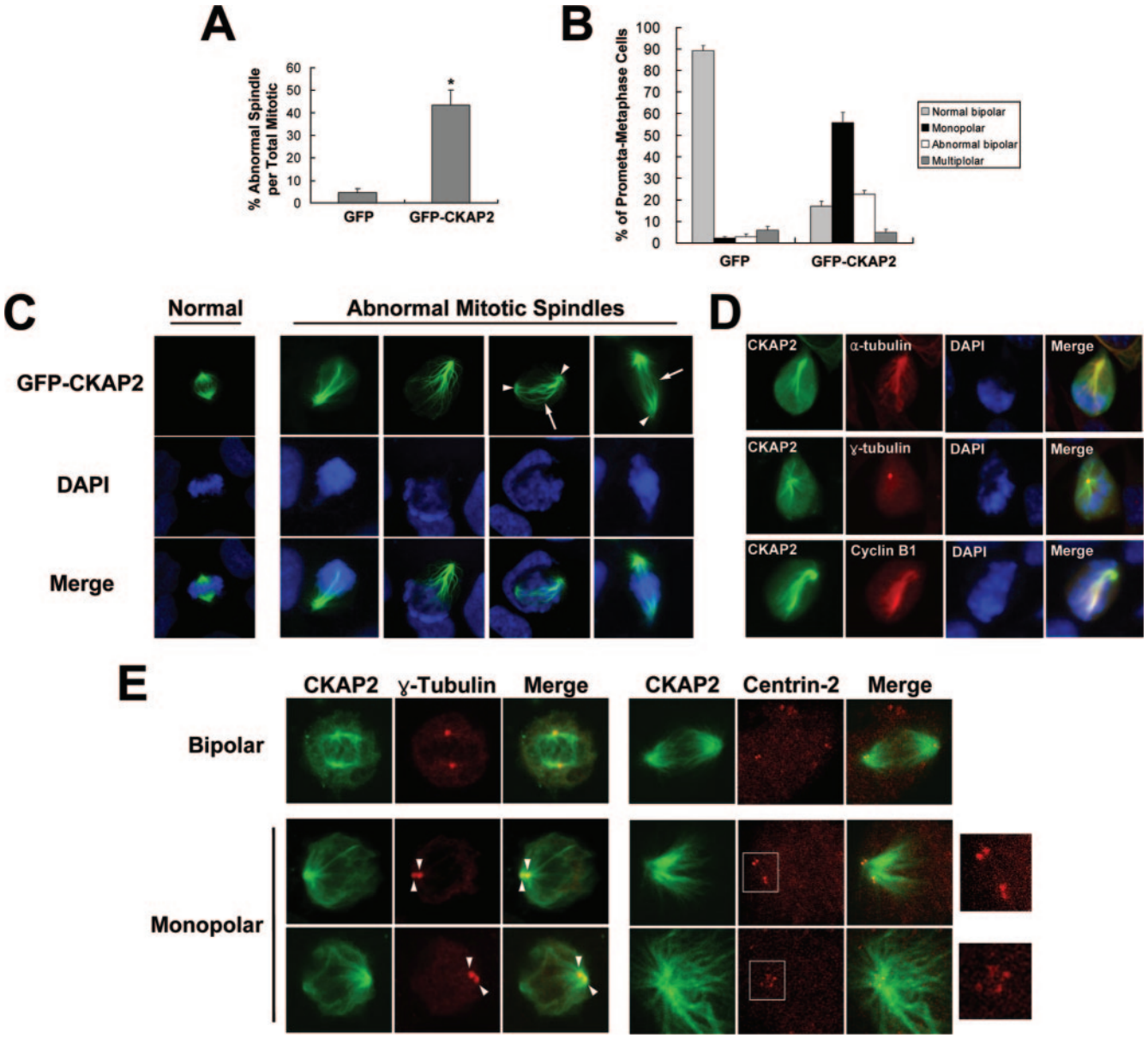

FIG. 3. Overexpression of TMAP/CKAP2 results in formation of spindle abnormalities due to a defect in centrosome separation. (A) Quantitative analysis of the percentage of mitotic cells with abnormal spindles among GFP- or GFP-CKAP2-expressing HEK 293A. HEK 293 cells were transfected with GFP (control) or GFP-CKAP2 and, after 2 days, fixed and immunostained for α-tubulin to visualize microtubules (not shown). The bar graphs show the mean values ± standard errors of the means, calculated as follows: (number of mitotic cells with abnormal spindles/total number of GFP-positive mitotic cells) × 100 (%). *, $P < 0.0001$. (B) Quantitative analysis of normal and different types of abnormal spindles among GFP- or GFP-CKAP2-expressing HEK 293 cells. Cells described in panel A were used for the analysis. Spindles in each GFP-positive mitotic cell were categorized into normal bipolar, monopolar, abnormal bipolar, or multipolar (having more than two spindles). Each bar graph shows the mean value ± standard error of the means, calculated as follows: (number of each spindle type/total number of GFP-positive mitotic cells) × 100 (%). Formation of a monopolar spindle was the most prevalent spindle defect in GFP-CKAP2-expressing cells. (C) Spindle defects in TMAP/CKAP2-overexpressing mitotic cells. HEK 293 cells were transfected with GFP (control; not shown) or GFP-CKAP2 and, after 2 days, fixed and counterstained with DAPI (blue). Representative images of monopolar and abnormal bipolar spindles are shown. Abnormal bipolar spindles were often characterized by having diffuse or nondistinct spindle poles (arrowheads) and long and well-developed interpolar microtubules (arrows). (D) Characterization of monopolar spindles formed within TMAP/CKAP2-overexpressing mitotic cells. HEK 293 cells were transfected with GFP-CKAP2 and, after 2 days, immunostained for α-tubulin, γ-tubulin, or cyclin B1 (red). Representative images of mitotic cells with monopolar spindles are shown. (E) Monopolar spindle formation in TMAP/CKAP2-overexpressing cells occurs due to a defect in centrosome separation. HEK 293 cells transfected with GFP-CKAP2 were immunostained for γ-tubulin (red), a centrosome-specific marker, or centrin-2 (red), a centriole-specific marker, to precisely identify the number of centrosomes at each spindle pole. Two centrosomes are either fused or unseparated (arrowheads) in cells forming monopolar spindles. Consistently, two pairs of centrioles are clearly present at a single spindle pole. The areas marked by the white boxes are magnified on the right.

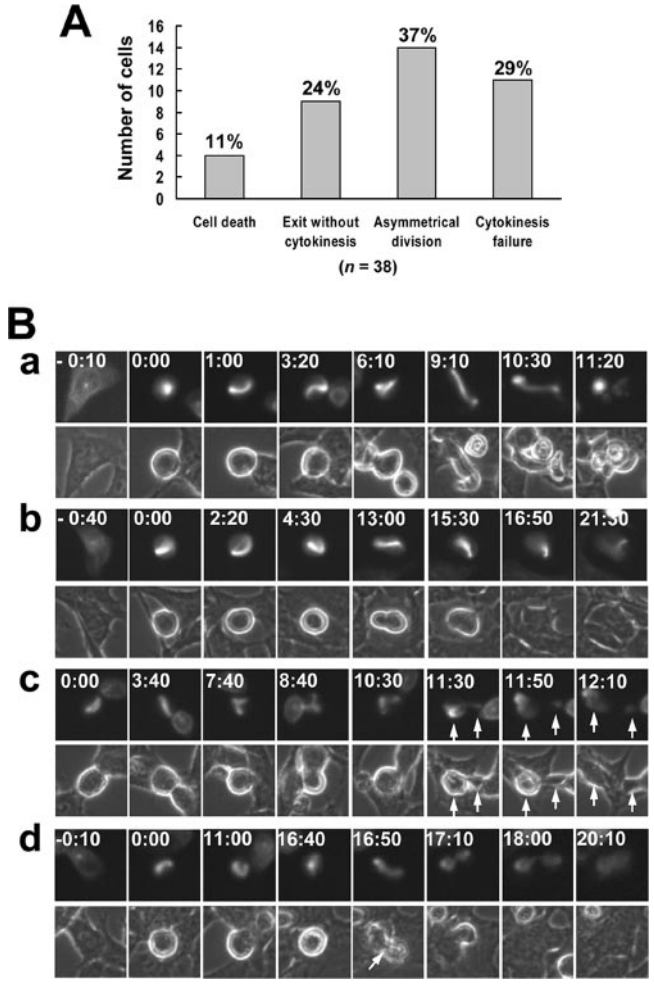

FIG. 4. Fate of TMAP/CKAP2-overexpressing cells developing spindle defects. HEK 293 cells transfected with GFP-CKAP2 were observed for 48 h using a time-lapse video microscope as described in Materials and Methods. (A) A total of 38 individual GFP-CKAP2-positive cells developing spindle defects (predominantly monopolar spindle formation) were continuously observed to assess their fate, which fell into the following four categories: cell death, exit without cytokinesis, asymmetrical division, and cytokinesis failure. (B) Representative time-lapse images (bright field and fluorescent) of a GFP-CKAP2-overexpressing cell undergoing cell death (a), exit without cytokinesis (b), asymmetrical division (c), or cytokinesis failure (d) after being arrested at a prometaphase-like state for a prolonged period of time. The numbers shown in the upper left corner indicate the relative passage of time (h:min). Interestingly, despite the spindle defect, a proportion of these cells (39%) eventually attempted to undergo a cell division, which resulted in an asymmetrical division of nuclear and cell material (c, arrows). However, approximately half of these cells (53%) either exited without cytokinesis (b) or initiated yet failed cytokinesis (d), resulting in tetraploid cells.

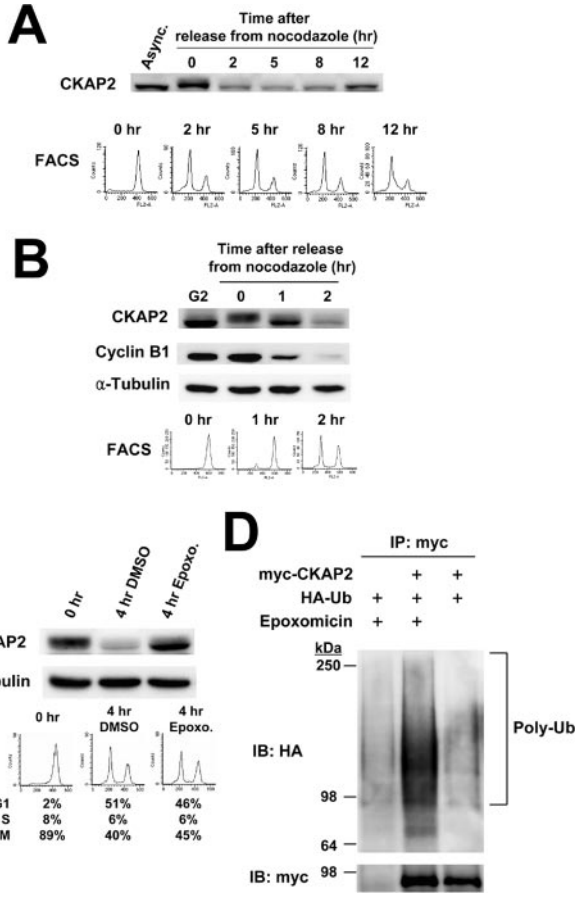

FIG. 5. TMAP/CKAP2 is rapidly degraded during mitotic exit via the ubiquitin-proteasome pathway. (A) TMAP/CKAP2 is degraded during mitotic exit. HeLa cells arrested at mitosis by nocodazole treatment (0 h) were released into nocodazole-free medium and analyzed at indicated time points by Western blotting (for TMAP/CKAP2) and FACS. (B) TMAP/CKAP2 is degraded during late mitosis and/or early G_1. HeLa cells arrested at mitosis by nocodazole treatment (0 h) were released into nocodazole-free medium and analyzed at 1-h and 2-h time points by Western blotting (for TMAP/CKAP2, cyclin B1, and α-tubulin) and FACS. Immunoblotting for cyclin B1 was performed in parallel to compare the timing of its destruction to that of TMAP/CKAP2. (C) Degradation of TMAP/CKAP2 is proteasome dependent. Nocodazole-arrested mitotic HeLa cells were released into fresh medium containing DMSO (vehicle control) or 500 nM epoxomicin, a proteasome inhibitor, for 4 h and analyzed by Western blot analysis (for TMAP/CKAP2 and α-tubulin) and FACS. (D) TMAP/CKAP2 is ubiquitylated in vivo. HEK 293T cells transfected with HA-ubiquitin (HA-Ub) alone or cotransfected with HA-ubiquitin and myc-tagged TMAP/CKAP2 (myc-CKAP2) were treated with or without epoxomicin. myc-CKAP2 was immunoprecipitated using a myc antibody. The immunoprecipitated samples were then resolved by SDS-PAGE and immunoblotted for myc and HA to detect immunoprecipitated myc-CKAP2 and high-molecular-weight, polyubiquitylated (Poly-Ub) myc-CKAP2, respectively. IB, immunoblot.

vested at indicated time points and analyzed by Western blotting and FACS analysis. As shown in Fig. 5A, the level of TMAP/CKAP2 protein rapidly declined during the first 2 h of release as cells exited from mitosis and entered into the G_1 phase. Its level remained low until the cells started to reenter the S phase of the cell cycle, in accordance with the findings of our previous study (22). Moreover, a closer analysis of the kinetics of TMAP/CKAP2 degradation revealed that its destruction was preceded by that of cyclin B1, the degradation of which is initiated during the transition from metaphase to anaphase (8) (Fig. 5B), which suggests that the degradation of TMAP/CKAP2 occurs during late mitosis and/or early G_1.

Such a rapid decline in the protein level suggested an active proteolytic mechanism, such as ubiquitylation and proteasome-mediated protein degradation (46). To test whether TMAP/

CKAP2 degradation during mitotic exit is proteasome dependent, nocodazole-arrested HeLa cells were treated with epoxomicin, a specific proteasome inhibitor (31), or DMSO as a vehicle control for 4 h as they were released into fresh medium. Epoxomicin treatment efficiently blocked the degradation of TMAP/CKAP2 during mitotic exit (Fig. 5C), indicating that the degradation is, in fact, proteasome dependent. FACS analysis performed in parallel indicated that the epoxomicin protocol used for the experiment did not significantly affect the kinetics of mitotic exit following nocodazole release (Fig. 5C). In other words, the inhibition of TMAP/CKAP2 degradation by epoxomicin treatment was not a result of gross inhibition of mitotic progression or exit. Next, we attempted to determine whether TMAP/CKAP2 is ubiquitylated in vivo. For the in vivo ubiquitylation experiment, HeLa cells were cotransfected with myc-tagged TMAP/CKAP2 (myc-CKAP2) and HA-tagged ubiquitin (HA-ubiquitin) or transfected with HA-ubiquitin alone. On the following day, cells were treated with epoxomicin or with DMSO alone for 6 h and harvested. myc-CKAP2 was then immunoprecipitated, and the presence of polyubiquitylated myc-CKAP2 was assessed by immunoblotting for HA-ubiquitin. The increased level of high-molecular-weight, HA-ubiquitin-conjugated protein bands or smear in the myc-CKAP2 immunoprecipitate indicated that TMAP/CKAP2 is indeed ubiquitylated in vivo (Fig. 5D). Additionally, the dependency of TMAP/CKAP2 degradation on proteasome has been also confirmed in other cell types, including U2OS, HEK 293, and NIH 3T3 (data not shown), indicating that it is not a cell-type-specific phenomenon. Taken together, these results demonstrate that TMAP/CKAP2 is actively degraded via the ubiquitin-proteasome pathway as cells exit from mitosis.

Degradation of TMAP/CKAP2 is mediated by APC-Cdh1. The timing of TMAP/CKAP2 degradation led us to hypothesize that it is mediated by the APC, which serves an important function of regulating degradation of various mitotic regulators (17). It has been previously shown that ectopic overexpression of Cdh1 and Cdc20, two known coactivators of APC, is able to induce the degradation of their substrates in a cell cycle-independent manner (2, 26). Based on this, we examined the degradation of TMAP/CKAP2 following ectopic overexpression of Cdh1 and Cdc20 in HeLa cells by cotransfecting them with GFP-CKAP2 and myc vector (control), myc-Cdh1, or myc-Cdc20. As shown in Fig. 6A, the introduction of Cdh1 resulted in a significant reduction in the level of GFP-CKAP2, as well as the level of endogenous TMAP/CKAP2, in a dose-dependent manner. In contrast, Cdc20 had no effect on the TMAP/CKAP2 protein level (Fig. 6A). Although overexpression of Cdh1 resulted in a slight increase in the G_0/G_1 population (Fig. 6A) and might have indirectly caused a decrease in the level of endogenous TMAP/CKAP2, it is unlikely that this increase the G_0/G_1 population affected the level of the exogenously introduced GFP-CKAP2 since its expression is driven by a CMV promoter. Next, we silenced Cdh1 using siRNA and examined its effect on the protein level of TMAP/CKAP2 during mitotic exit. HeLa cells transfected with a plasmid expressing shRNA for Cdh1 showed a decreased level of Cdh1 compared to the control shRNA-transfected cells (Fig. 6B). Silencing Cdh1 significantly inhibited the degradation of TMAP/CKAP2, as well as Aurora B, Plk1, and cyclin B1, previously known substrates of APC-Cdh1 (12, 28, 32, 41), during mitotic exit (Fig. 6B). The differences in the level of inhibition can be attributed to the fact that degradation of Aurora B, Plk1, and cyclin B1 is also mediated by APC-Cdc20 (12, 32). Additionally, the introduction of a dominant negative mutant of Cdh1 which corresponded to the substrate-binding region at the N terminus (i.e., the first 125 aa) (26, 36) efficiently inhibited degradation of exogenously introduced GFP-CKAP2, as well as endogenous TMAP/CKAP2, during mitotic exit (data not shown). These results demonstrate that Cdh1 is required for degradation of TMAP/CKAP2 to occur during the transition from mitosis to G_1. Consistent with this conclusion, the timing of TMAP/CKAP2 degradation examined by Western blotting and time-lapse video microscopy coincided with the window of Cdh1 activation, i.e., late mitosis through early G_1 (40, 44) (Fig. 5B and 7F).

However, it was still possible that the TMAP/CKAP2 protein level is indirectly affected by Cdh1. Thus, in order to demonstrate that TMAP/CKAP2 is a direct substrate of APC-Cdh1 complex, we first examined the in vivo interaction between TMAP/CKAP2 and Cdh1. As shown in Fig. 6C, TMAP/CKAP2 was successfully coimmunoprecipitated with myc-Cdh1 and vice versa, which indicated that an interaction does occur in vivo. In contrast, the in vivo interaction between TMAP/CKAP2 and Cdc20 could not be detected by the coimmunoprecipitation assay (see Fig. S3 in the supplemental material). Next, an in vitro ubiquitylation assay was carried out. For the assay, the APC was partially purified from the lysate of nocodazole-arrested, mitotic HeLa cells by immunoprecipitation using a monoclonal antibody against Cdc27. Nus-tagged TMAP/CKAP2 (Nus-CKAP2) was incubated with immunopurified mitotic APC and recombinant Cdh1 in the presence of ubiquitin, ubiquitin aldehyde, and an energy regenerating system. As shown in Fig. 6D, high-molecular-weight, polyubiquitylated Nus-CKAP2 was clearly present in the reaction containing both APC and Cdh1; occurring concomitantly with the increase in polyubiquitylated Nus-CKAP2, there was a decrease in the level of unmodified Nus-CKAP2, indicating that TMAP/CKAP2 is directly ubiquitylated by APC-Cdh1. Taken together, these results demonstrate that TMAP/CKAP2 is a novel substrate of the APC-Cdh1 complex by which it is ubiquitylated and targeted to proteasome-dependent degradation during mitotic exit.

The KEN box motif is required for degradation of TMAP/CKAP2. We next sought to identify destruction motifs that mediate the degradation of TMAP/CKAP2. First, various myc-tagged deletion mutants of TMAP/CKAP2 were examined for degradability in order to identify a region required for its degradation. Each of the deletion mutants was cotransfected into HeLa cells with GFP-full-length CKAP2 to allow assessment of its degradability relative to that of the full-length TMAP/CKAP2 during release from the nocodazole block. Also, in order to avoid the possibility of saturating the cellular degradation machinery, the amount of DNA used for transfection was adjusted so that the expression level of the deletion mutants was comparable to that of endogenous TMAP/CKAP2 (data not shown). The full-length TMAP/CKAP2 and a C terminus deletion mutant lacking residues 458 to 682, CKAP2Δ458–682, were both efficiently degraded during mitotic exit, whereas a N terminus deletion mutant, CKAP2Δ1–

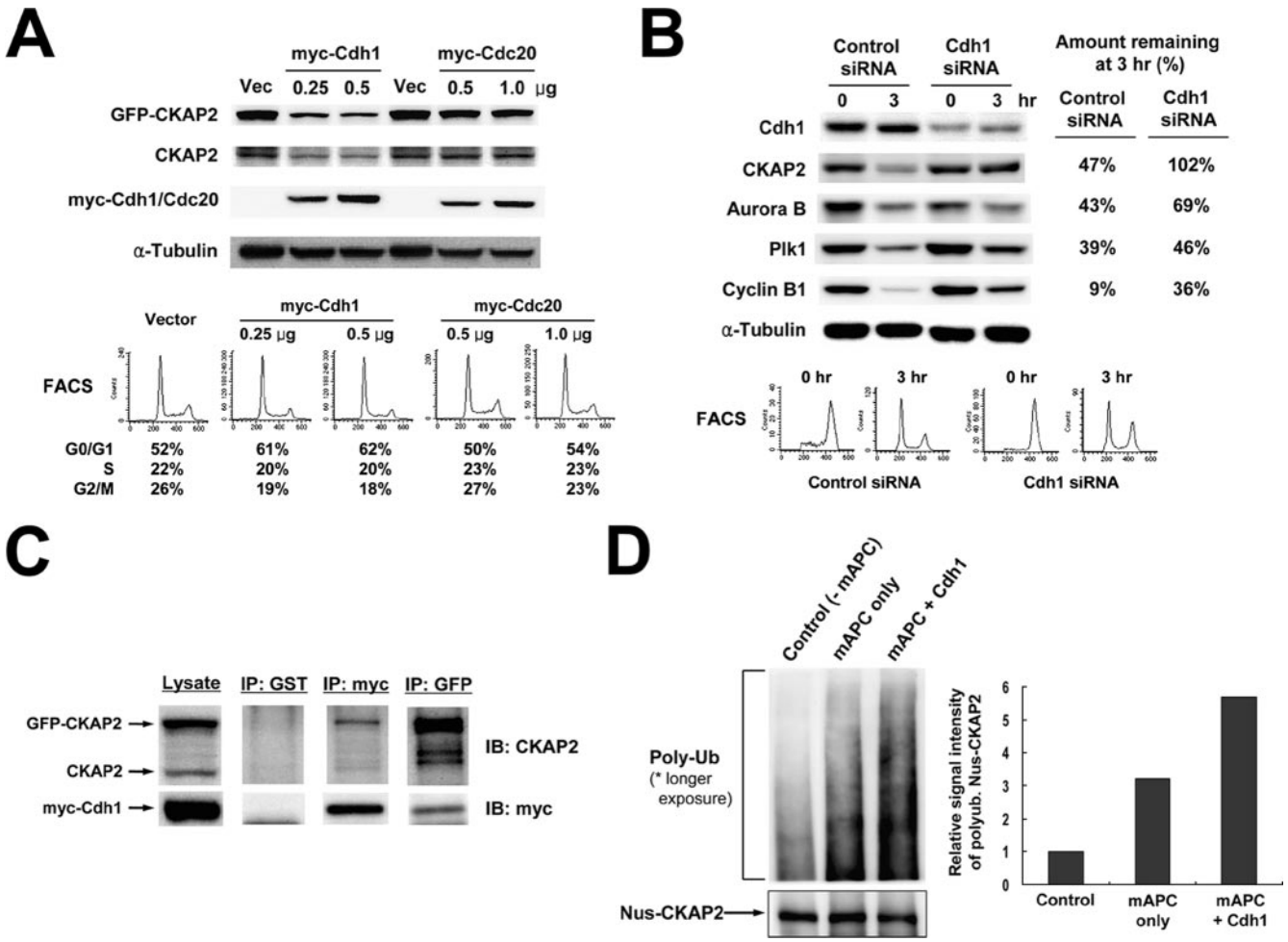

FIG. 6. Degradation of TMAP/CKAP2 during mitotic exit is mediated by APC-Cdh1. (A) Ectopic overexpression of Cdh1 induces cell cycle-independent degradation of TMAP/CKAP2. HeLa cells were cotransfected with GFP-CKAP2 and various amounts of myc-Cdh1 or myc-Cdc20 and were harvested on the following day and analyzed by Western blotting (for TMAP/CKAP2, myc, and α-tubulin) and FACS analysis. (B) Silencing Cdh1 prevents degradation of TMAP/CKAP2 during mitotic exit. HeLa cells transfected with control or Cdh1 siRNA were arrested at mitosis by nocodazole treatment (0 h) and released into fresh medium for 3 h (3 h). Protein levels of Cdh1, TMAP/CKAP2, Aurora B, Plk1, cyclin B1, and α-tubulin were assayed by Western blot analysis (left). The cell cycle profile of each sample determined by FACS is shown below. The intensities of the protein bands shown in the left panel were quantified, and the amount remaining at 3 h of nocodazole release was expressed as a percentage of the starting amount at time zero (right). (C) Interaction between TMAP/CKAP2 and Cdh1 in vivo. HeLa cells were cotransfected with GFP-CKAP2 and myc-Cdh1. myc-Cdh1 or GFP-CKAP2 was immunoprecipitated using an antibody against c-*myc* or GFP, respectively, and the presence of coimmunoprecipitated GFP-CKAP2 and endogenous TMAP/CKAP2 or myc-Cdh1 was assayed by Western blot analysis. An antibody against GST was used as an IgG or negative control for the assay. IB, immunoblot. (D) In vitro ubiquitylation assay. Purified Nus-tagged TMAP/CKAP2 was incubated with immunopurified mitotic APC (mAPC) in the presence of E1 ligase, UbcH10 (E2), ubiquitin, ubiquitin aldehyde, the ATP regenerating system, and recombinant Cdh1 (mAPC+Cdh1) (left). For the negative control reactions, either mitotic APC (−mAPC) or Cdh1 (mAPC only) was omitted from the reaction. The in vitro reaction products were then analyzed for the level of input substrate (i.e., Nus-CKAP2) and high-molecular-weight polyubiquitylated (Poly-Ub) substrate by Western blot analysis. The upper portion of the blot was exposed for a longer period to detect Poly-Ub substrate. At right is the quantification of the intensity of polyubiquitylated Nus-CKAP2 smear shown on the left panel. Intensity of the high-molecular-weight, polyubiquitylated band smear of each lane was quantified and background subtracted using Multi Gauge (version 3.0) software (Fujifilm). The intensity of the control lane was set as the reference value (i.e., 1) to allow assessment of relative changes in the band intensity.

263 was resistant to degradation, indicating that at least one destruction motif resided near the N terminus, i.e., within the first 263 amino acids (Fig. 7A). Consistent with this result, the N-terminal fragment, i.e., CKAP2Δ264–682, alone was efficiently degraded (Fig. 7A).

It is well known that the substrates of the APC share common destruction motifs, namely, the D box (RXXL) and KEN box. The D box can be recognized by both Cdc20 and Cdh1, whereas the KEN box is recognized by only Cdh1 (6, 36). Analysis of the sequences of the first 263 aa of TMAP/CKAP2 revealed several putative D boxes and one KEN box. Unlike putative D boxes, the KEN box, located at aa 80 to 82, was well conserved among higher eukaryotes (Fig. 7B). Thus, we hypothesized that the KEN box serves as the destruction motif for TMAP/CKAP2. To test this hypothesis, a KEN box mutant of TMAP/CKAP2 in which all three residues were replaced

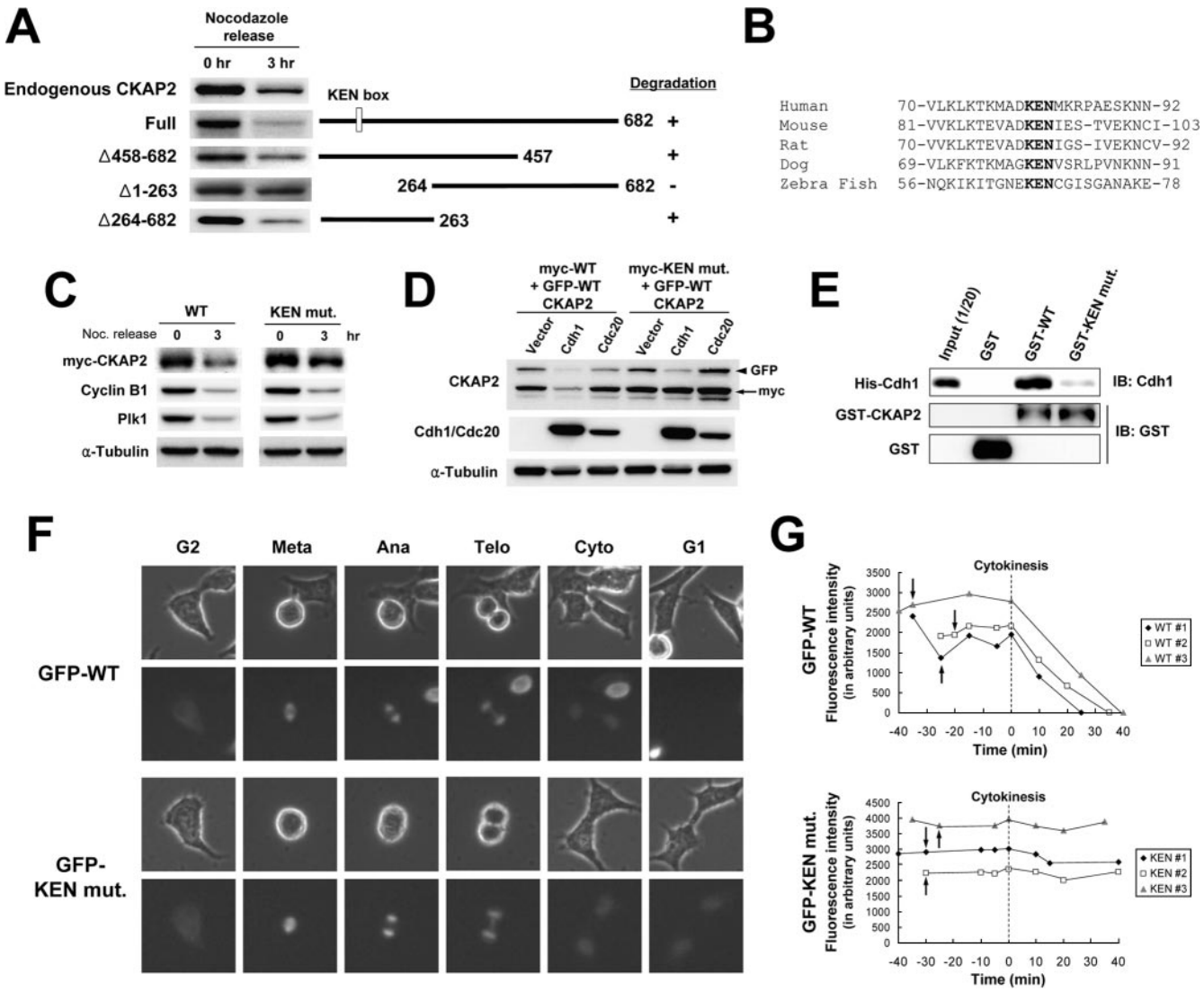

FIG. 7. Degradation of TMAP/CKAP2 is mediated by the KEN box destruction motif located near the N terminus. (A) Degradability of deletion mutants of TMAP/CKAP2 during mitotic exit. HeLa cells transfected with the myc-tagged full-length or indicated deletion mutants of TMAP/CKAP2 were arrested at mitosis by nocodazole treatment (0 h), released into fresh medium, and analyzed 3 h later by Western blot analysis using a polyclonal antibody against TMAP/CKAP2. The right panel shows a summary diagram indicating the types of deletion mutants analyzed and their degradability during mitotic exit. The white box marks the location of the KEN box (aa 80 to 82). (B) A KEN box destruction motif is located near the N terminus of TMAP/CKAP2 and is conserved among higher eukaryotes. The panel shows the alignment of amino acid sequences of the KEN box-containing N-terminal portion of TMAP/CKAP2 in different species. The KEN box is highlighted in bold. (C) The KEN box mutant of TMAP/CKAP2 is resistant to degradation during mitotic exit. HeLa cells were transfected with myc-WT or myc-KENmut TMAP/CKAP2, in which all three residues had been replaced with alanines, arrested at mitosis by nocodazole treatment (0 h), and released into fresh medium for 3 h. The cells were then analyzed for changes in the levels of myc-tagged WT or KENmut TMAP/CKAP2, Plk1, cyclin B1, and α-tubulin by Western blot analysis. (D) The KEN box is required for Cdh1-mediated degradation of TMAP/CKAP2. myc-WT or KENmut TMAP/CKAP2 was cotransfected into HeLa cells with GFP-WT CKAP2 and myc vector, myc-Cdh1, or myc-Cdc20. The cells were harvested on the following day and analyzed by Western blot analysis as shown. Arrow, myc-WT or -KENmut CKAP2 protein band; arrowhead, GFP-WT CKAP2 protein band. (E) In vitro GST pull-down assay showing that interaction between TMAP/CKAP2 and Cdh1 is dependent on the KEN box. Glutathione-Sepharose beads bound to recombinant GST (control) or GST-WT or GST-KENmut TMAP/CKAP2 were incubated with recombinant His-tagged Cdh1 (His-Cdh1). Proteins bound to beads were resolved by SDS-PAGE and immunoblotted for Cdh1 and GST to detect coprecipitated His-Cdh1 and GST or GST-WT/KENmut, respectively. IB, immunoblot. (F) Analysis of WT and KENmut TMAP/CKAP2 by time-lapse video microscopy. HEK 293 cells were transfected with GFP-WT or GFP-KENmut CKAP2 and observed using time-lapse video microscopy. A representative cell expressing each construct is shown at the indicated stages of the cell cycle. Both bright-field and fluorescence images were acquired under a magnification of ×200 at 5-min intervals. (G) Quantitative analysis of changes in the fluorescence intensity of GFP-WT and GFP-KENmut CKAP2 during and after mitosis. Cells described in panel F were used for the analysis. For each construct, the intensity of GFP fluorescence (indicative of the protein level) was measured during mitosis and early G_1 in three representative cells. The time at which each cell entered cytokinesis was used as a reference point (time zero) which is indicated by a dashed line. The arrows mark the point at which the cells entered pro/prometaphase. While the level of WT protein declines rapidly after cells initiate cytokinesis and enter into G_1, the level of KENmut protein persists throughout and after mitosis.

with alanines (i.e., ^{80}KEN^{82} to ^{80}AAA^{82}) (KENmut) was generated and tested for degradability during mitotic exit and by ectopic overexpression of Cdh1 and Cdc20. The mutation in the KEN box significantly reduced degradation of the full-length protein (Fig. 7C). In contrast, mutations in putative D boxes (i.e., ^{27}RQKL^{30}, ^{37}RKTL^{40}, and ^{554}RNLL^{557}) did not affect the degradation of TMAP/CKAP2 (data not shown). Moreover, the KEN box mutant was completely resistant to degradation induced by ectopic overexpression of Cdh1, unlike its WT counterpart (Fig. 7D). In support of these findings, an in vitro GST pull-down assay demonstrated that the mutation in the KEN box alone was sufficient to strongly diminish the interaction between TMAP/CKAP2 and Cdh1 (Fig. 7E). This finding is consistent with a previous report that the KEN box directly mediates the interaction between Cdh1 and its KEN box-dependent substrates (36). Furthermore, analysis of HEK 293 cells transfected with either GFP-WT or GFP-KENmut TMAP/CKAP2 by time-lapse video microscopy finally showed that the KENmut TMAP/CKAP2 protein persisted through and beyond mitosis, whereas the WT protein started to disappear upon initiation of cytokinesis and became undetectable in G_1 (Fig. 7F). Quantification of the GFP fluorescence of WT or KENmut protein before, during, and after mitosis also confirmed the observation that the mutation in the KEN box rendered the full-length protein completely resistant to degradation during mitotic exit (Fig. 7G). These data demonstrate that the KEN box located near the N terminus serves as the major destruction motif and is required for the degradation of TMAP/CKAP2 during mitotic exit.

Degradation of TMAP/CKAP2 is important for establishment of spindle bipolarity and completion of cytokinesis. Next, we questioned whether degradation of TMAP/CKAP2 during mitotic exit is of any functional significance. First, we postulated that failure to properly degrade TMAP/CKAP2 and subsequent accumulation of TMAP/CKAP2 would influence microtubule dynamics by increasing microtubule stability, especially during the early stages of mitosis. This would ultimately result in the spindle abnormalities observed following TMAP/CKAP2 overexpression. However, it proved difficult to address this because KENmut constructs always generated higher levels of the protein than the WT due to its nondegradable nature. As a result, the KENmut construct always induced a higher frequency of spindle defects when transiently transfected (data not shown). So, whenever we attempted to compare the effects of the KENmut expression at the population level by FACS analysis or by measuring the increase in the mitotic index, for instance, we were not able to distinguish the effect of the protein's being stable during mitotic exit from the effect of simply higher protein expression. Thus, in order to study the importance of protein stability during mitotic exit, it was necessary to ensure that the cellular levels of the WT protein and the KENmut counterpart were the same (or at least similar) as cells entered and exited mitosis. We decided to examine the fate of individual cells expressing GFP-WT or GFP-KENmut TMAP/CKAP2. First, we transiently transfected HEK 293 cells with either GFP-WT or GFP-KENmut TMAP/CKAP2 and observed them using time-lapse video microscopy. Since an elevated level of either WT or KENmut TMAP/CKAP2 results in formation of spindle defects and prevents proper progression through mitosis, we focused on GFP-WT- or GFP-KENmut-expressing cells that satisfied the following criteria: (i) formation of normal bipolar spindle structure and (ii) progression into anaphase and the rest of the mitotic phases without significant delays. Based on formation of normal bipolar spindle and normal progression through mitosis, we reasoned that these cells expressed the GFP fusion protein at a similar and nonexcessive level. To demonstrate this quantitatively, we measured the fluorescence intensity, which positively correlates with the level of GFP fusion protein expressed, of individual cells analyzed in the experiment when they reached metaphase of the first round of the cell cycle. The result showed that the cells which satisfied the above criteria were indeed expressing similar levels of the GFP fusion protein, regardless of the type of construct (i.e., WT or KENmut) used for transfection (Fig. 8A). We then continuously observed these cells as they successfully completed the first round of mitosis and progressed through the next cell cycle. In the case of cells expressing the WT TMAP/CKAP2, the majority (9 out of 10) of those that successfully completed the first round of mitosis were also successful in entering and completing the second round. However, more than half of the cells expressing the nondegradable KENmut (7 out of 12), which had accumulated GFP-KENmut TMAP/CKAP2 from the first round, either exhibited a prolonged mitosis (>4 h) or failed to complete the second round of mitosis normally due to the development of spindle defects upon entry into mitosis (Fig. 8A). This observation indicates that degradation of TMAP/CKAP2 during mitotic exit is necessary for proper establishment and maintenance of spindle bipolarity in subsequent cell cycles.

Additionally, while we were examining the time-lapse video microscopy data, we observed that, interestingly, a number of cells expressing the KENmut TMAP/CKAP2 frequently failed to divide into two daughter cells, resulting in binucleate, tetraploid cells; in spite of that, they satisfied the criteria described above (i.e., absence of any observable spindle defects or significant delays in the mitotic progression). Closer examination of these cells revealed that fusion of two daughter cells resulted from an incomplete cytokinesis rather than failure to initiate cytokinesis (Fig. 8B). In order to quantitatively compare the frequency of such cytokinesis failure between WT- and KENmut-expressing cells, we analyzed HEK 293 cells transiently transfected with GFP-WT or GFP-KENmut TMAP/CKAP2, applying the same criteria used for the experiment described above. According to the results of four independently performed experiments, the frequency of reversed or incomplete cytokinesis among GFP-KENmut TMAP/CKAP2-expressing cells was approximately four times higher than that in the GFP-WT-expressing control cells (Fig. 8B; see Table S1 in the supplemental material). It should be emphasized that the cells analyzed here expressed similar and nonexcessive levels of the GFP fusion protein, and, therefore, the difference in the frequency of cytokinesis failure between WT and KENmut cannot simply be attributed to a difference in the level of protein expression. These results indicate that degradation of TMAP/CKAP2 during mitotic exit is important not only for maintenance of spindle bipolarity during mitosis but also for proper completion of cytokinesis.

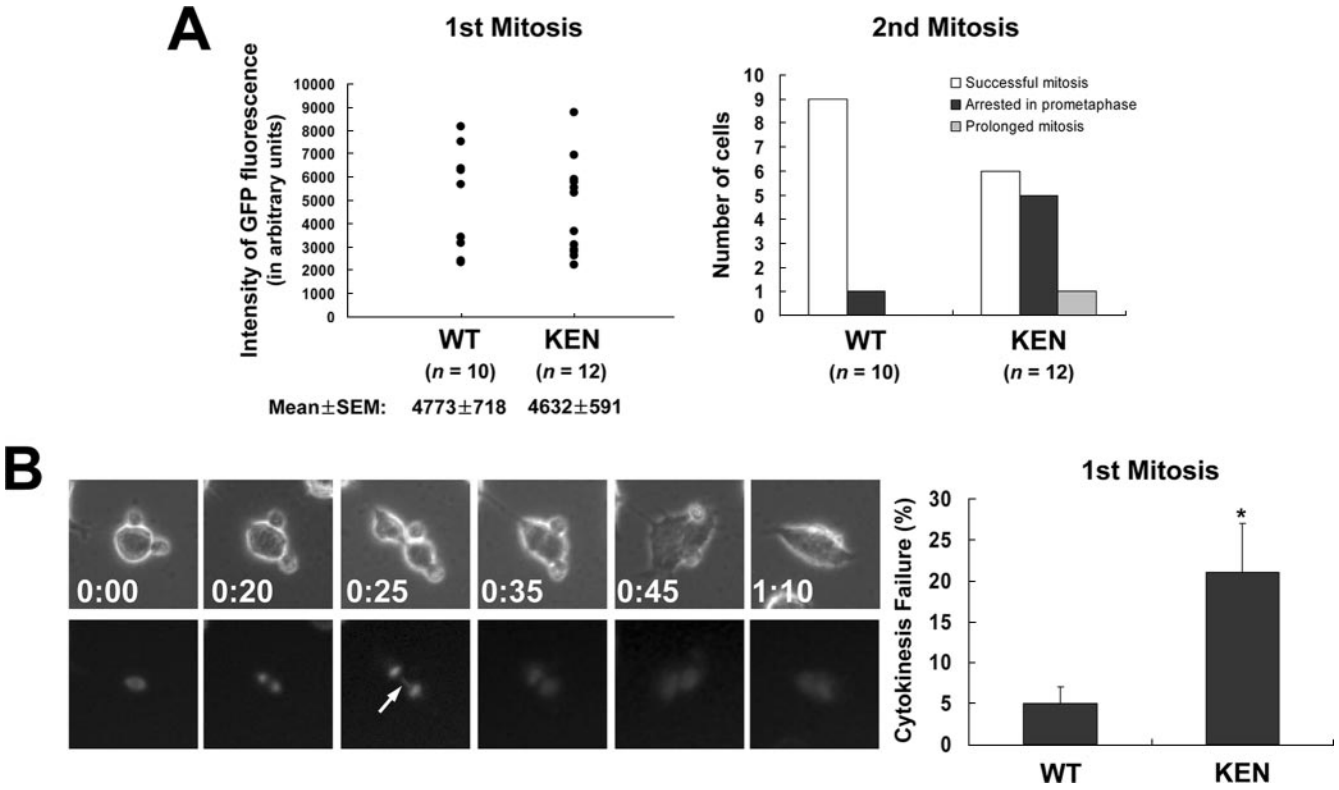

FIG. 8. Expression of nondegradable KENmut TMAP/CKAP2 results in the formation of spindle defects and failure of cytokinesis. (A) HEK 293 cells were transfected with GFP-WT CKAP2 (WT) or GFP-KENmut CKAP2 (KEN) and were observed using time-lapse video microscopy. GFP-CKAP-expressing cells that successfully progressed through the first round of mitosis (i.e., without any spindle defects or significant delays in mitotic progression) were followed throughout the next cell cycle and examined for formation of any mitotic spindle defects and subsequent arrest at prometaphase in the second mitosis. The left panel shows the intensity of GFP fluorescence (indicative of the protein level) in cells expressing GFP-WT or GFP-KENmut as cells reached metaphase of the first mitosis, which indicates that the cells selected for this analysis were expressing a similar level of GFP fusion proteins. The right panel shows the frequency of cells exhibiting successful mitosis, prometaphase arrest due to formation of spindle defects (arrested in prometaphase), or significant delays (>4 h) in mitotic progression (prolonged mitosis) among GFP-WT- or GFP-KENmut-expressing cells shown in the left panel. Compared to the WT, expression of nondegradable KENmut TMAP/CKAP2 resulted in an increased frequency of mitotic arrest in the following round of the cell cycle due to the formation of mitotic spindle defects, typified by formation of monopolar spindles. *n*, number of cells analyzed; SEM, standard error of the mean. (B) Increased frequency of cytokinesis failure among KENmut-expressing cells. Bright-field and GFP fluorescence images (left panel) show a GFP-KENmut-expressing HEK 293 cell that progresses through mitosis and initiates cytokinesis (at 0:25) yet fails to complete it, resulting in a binucleated cell. The arrow indicates GFP-KENmut localized to midbody microtubules. Numbers shown in the lower left corner indicate the relative passage of time (h:min). At right is a quantitative analysis of the percentage of cells undergoing cytokinesis failure among GFP-WT (WT)- and GFP-KENmut CKAP2 (KEN)-expressing cells that had successfully entered and progressed through mitosis (i.e., without any spindle defects or significant delays in mitotic progression). The bar graphs show the mean values ± standard error of the mean obtained from four independent experiments. The number of cells observed in each experiment ranged from 18 to 22 (see Table S1 in the supplemental material). *, $P < 0.05$.

DISCUSSION

We have previously shown the cell cycle-dependent changes in the level of TMAP/CKAP2 transcripts and protein using synchronized human foreskin fibroblasts, which implicated TMAP/CKAP2 in the G_2/M phases of the cell cycle (22). Such cell cycle-dependent changes in the level of TMAP/CKAP2 have also been supported by previous microarray studies that provided the gene expression profiles of cell cycle-regulated genes (21, 47). These studies have shown that in both HeLa cells and primary human fibroblasts, the level of TMAP/CKAP2 transcripts starts to rise near the G_1/S transition and peaks during the G_2/M phases. Interestingly, based on cluster analysis, it was found that TMAP/CKAP2 belonged to one of the G_2- and M-phase clusters (namely, "spindle assembly" cluster) along with a number of genes involved in the assembly and regulation of the mitotic spindle, including kinesin-like motor proteins (e.g., Eg5, KIF5, and CENP-E), mitotic kinases, and cyclins (e.g., Plk1, Aurora A and B kinases, Nek2, Cdk1, and cyclin B) (47). This finding suggests that the cellular functions of TMAP/CKAP2 pertain to mitotic events.

One of the most discernible consequences of TMAP/CKAP2 overexpression was the development of microtubule bundles, which was associated with increased stability of microtubules. Recently published studies on TMAP/CKAP2 have also reported that mTMAP/CKAP2 has microtubule-stabilizing properties and that overexpression of human TMAP/CKAP2 results in an increased level of acetylated tubulin, which is indicative of microtubule stabilization (23, 43). A number of microtubule-associated proteins (MAPs) with microtubule-stabilizing properties, e.g., MAP2, EB-1, CLIP-170, Doublecor-

tin, and NuSAP, have been shown to induce microtubule bundling upon overexpression (5, 19, 37, 38, 45). The patterns and shapes of microtubule bundles induced by TMAP/CKAP2 were highly similar to those induced by EB-1 and CLIP-170 (5, 37), microtubule plus-end binding proteins, in that bundled microtubules often formed continuous curvatures or circumferential rings around the cell periphery (see Fig. S2 in the supplemental material). However, the exact mechanism by which TMAP/CKAP2 enhances the stability of microtubules is not clear. Also, it is difficult to discern whether TMAP/CKAP2 indirectly affects microtubule stability by promoting microtubule bundling or microtubule bundling is a consequence of increased microtubule stability induced by TMAP/CKAP2. Our preliminary studies indicate that unlike the MAPs mentioned above, TMAP/CKAP2 does not appear to directly bind microtubules in vitro but requires the presence of MAPs for its association with microtubules (S.-M. Jeon, C.-D. Bae, and J. Park, unpublished data). Therefore, it is likely that TMAP/CKAP2 indirectly affects the stability of microtubules and/or cross-link microtubule polymers by interacting with microtubule-associated factors that regulate microtubule dynamics (see below).

Another interesting outcome of TMAP/CKAP2 overexpression observed in the present study was the formation of monopolar spindles that resulted in a significant increase in the mitotic index due to cell cycle arrest at mitosis. As a result, disorganized distribution and misalignment of sister chromatids were evident within these cells. The spindle checkpoint monitors the status of kinetochore-microtubule attachments and prevents cells from progressing to anaphase until all kinetochores are properly attached to microtubules (3). Thus, the prometaphase/metaphase arrest observed in TMAP/CKAP2-overexpressing cells with monopolar spindles is presumably due to activation of the spindle checkpoint. The relatively high level of cyclin B1 located along the spindles in these cells also indicates that they had not progressed to anaphase (Fig. 3D). Interestingly, even some of the mitotic cells with bipolar spindles exhibited abnormal spindle morphologies, and the sister chromatids still failed to congress, which suggests that in addition to the centrosome separation defects, mitotic spindle function itself is impaired in TMAP/CKAP2-overexpressing cells. Formation of unusually elongated and bundled microtubules in cells with monopolar or abnormal bipolar spindles suggests that these mitotic spindle defects result, at least in part, from the increased stability of microtubules induced by TMAP/CKAP2.

Monopolar spindles induced by TMAP/CKAP2 overexpression were caused by a defect in centrosome separation. Centrosomes duplicated prior to mitosis must separate at the onset of mitosis in order to establish bipolar mitotic spindles (10). However, relatively little is known about the process of centrosome separation. It has been suggested that at least two independent pathways contribute to spindle bipolarity: the Eg5/BimC-dependent pathway using motor force and the pathway relying on microtubule polymer dynamics that involve microtubule stabilizing and destabilizing kinesin-like proteins (14, 27). Both of these pathways are critical to the induction of centrosome separation and the establishment of spindle bipolarity, as disruption or depletion of the factors involved in these pathways results in monopolar spindle formation (14, 16, 20, 25, 29, 48). Interestingly, there were noticeable similarities between the spindle defects observed in TMAP/CKAP2-overexpressing cells and the defects induced by depletion of KIF2a and Klp67A/KIF18; in both cases, monopolar or abnormal bipolar spindles with elongated microtubules and diffuse spindle poles were observed (14, 16, 48). Thus, it is possible that endogenous TMAP/CKAP2 may influence microtubule dynamics and thus spindle bipolarity by negatively regulating these microtubule-destabilizing kinesin-related proteins during mitosis.

TMAP/CKAP2 is a novel substrate of the APC-Cdh1 complex. In addition to securin and mitotic cyclins, which are some of the most extensively studied substrates of the APC, the proteins that are targeted for destruction by the APC are quite diverse (17). Some of these substrates include proteins involved in spindle function, such as the anaphase spindle elongation control protein, Ase1 (24), the kinesin-like proteins (e.g., Cin8 and Kip1 [BimC/Eg5] [15, 18], CENP-E [4], and Xkid/Nod [7]), and a recently discovered substrate, shugoshin (39), indicating that the APC also plays an important role in regulating spindle assembly, dynamics, and disassembly as well as chromosome movements. It has been proposed that degradation of the proteins involved in spindle function provides a mechanism for resetting their activity to a low, premitotic state prior to the spindle assembly in the following cell cycle (17, 18). Similarly, degradation of TMAP/CKAP2 by the APC may play a role in regulating the spindle function and its disassembly upon mitotic exit. This notion is supported by the results of the present study, as introduction of a nondegradable mutant of TMAP/CKAP2 resulted in a significant increase in the frequency of spindle defects in the subsequent round of mitosis compared to the WT (Fig. 8A).

Another major, and perhaps more important, consequence of introducing a nondegradable mutant of TMAP/CKAP2 was a significant increase (fourfold) in the frequency of cytokinesis failures, which suggests that TMAP/CKAP2 is also involved in the process of cytokinesis either directly or indirectly and that proper regulation of the TMAP/CKAP2 level is required for the completion of cytokinesis. However, it is unclear from the currently available data how nondegradable TMAP/CKAP2 exerts its effect on cytokinesis. Although we cannot completely rule out the possibility that the effect of nondegradable TMAP/CKAP2 on the mitotic spindle during earlier phases of mitosis might have resulted in cytokinesis failure, we currently think that it may be independent from the spindle-related effect for the following reasons: (i) both GFP-WT- and GFP-KENmut-expressing cells examined for the experiment expressed similar and nonexcessive levels of the GFP fusion protein at the start of mitosis, established normal bipolar spindle structures, and progressed through mitosis without significant delays, which suggests that gross structural or functional defects in the spindle apparatus were absent; and (ii) by the time the cells initiated cytokinesis, the majority of TMAP/CKAP2 was no longer associated with spindle microtubules but, rather, localized to the newly formed daughter nuclei and to the midbody microtubules (Fig. 1 and Fig. 8B). This suggests that the cause of cytokinesis failures is not directly related to the spindle defects that result from an excessive level of TMAP/CKAP2. In support of this idea, we observed that few cells expressing similar levels of WT protein exhibited cytokinesis failures (Fig. 8B).

Although the exact nature and cause of the cytokinesis failure observed in these cells require further investigation, perhaps the persistence of nondegradable TMAP/CKAP2 at the midbody microtubules during cytokinesis might influence local microtubule dynamics and interfere with the final abscission process. Regardless of the underlying mechanism, the present finding implies that the APC also regulates the completion of cytokinesis by accomplishing the timely destruction of the factors involved in the process, including TMAP/CKAP2.

The findings of the present study appear somewhat contradictory to the previous reports that TMAP/CKAP2 is frequently upregulated in cancers (1, 11, 30) because the consequence of an increased TMAP/CKAP2 level should be detrimental rather than beneficial to cell growth and viability. However, it is possible that the increased level of TMAP/CKAP2 and subsequent deregulation of the spindle function may induce abnormal cell divisions (Fig. 4) and thus contribute to overall chromosome instability in tumor cells. Alternatively, the elevated level of TMAP/CKAP2 in cancers may simply reflect the abnormally high rates of cell proliferation. As discussed previously, the level of TMAP/CKAP2 expression is cell cycle regulated, and it remains low or absent in cells at G_0/G_1. Consistent with this, the level of TMAP/CKAP2 protein was low or undetectable in growth-arrested human primary foreskin fibroblasts and NIH 3T3 cells (22). Thus, the level of TMAP/CKAP2 is expected to be much higher in cancerous tissues where cell proliferation is robust than in relatively quiescent normal tissues. Additionally, it is possible that TMAP/CKAP2 provides growth and/or survival advantages to the cells in which it is expressed. Preliminary studies conducted in our laboratory have shown that overexpression of TMAP/CKAP2 at a moderate level actually promotes cell growth in human foreskin fibroblasts and NIH 3T3 cells (22) and also promotes cell survival as it provides resistance to apoptotic stimuli in a colorectal cancer cell line (B. Choi, K. U. Hong, C.-D. Bae, and J. Park, unpublished observations). These observations suggest that TMAP/CKAP2 may serve diverse functions.

In conclusion, based on the results of the present study, we propose that TMAP/CKAP2 functions in the assembly and maintenance of the mitotic spindle, presumably via regulation of microtubule dynamics during mitosis, and that its protein level needs to be properly regulated during the cell cycle to ensure establishment and maintenance of functional bipolar spindles as well as completion of cytokinesis. The precise roles of TMAP/CKAP2 in the maintenance of mitotic spindle and progression of mitotic events are currently under investigation using TMAP/CKAP2-specific siRNAs and TMAP/CKAP2 knockout mice.

ACKNOWLEDGMENTS

This work was supported by research grants from the National R&D Program for Cancer Control, Ministry of Health and Welfare, Republic of Korea (grant 0420220), and from the Molecular and Cellular Bio-Discovery Project, KISTEP (grant 2004-01789).

REFERENCES

1. **Bae, C. D., Y. S. Sung, S. M. Jeon, Y. Suh, H. K. Yang, Y. I. Kim, K. H. Park, J. Choi, G. Ahn, and J. Park.** 2003. Up-regulation of cytoskeletal-associated protein 2 in primary human gastric adenocarcinomas. J. Cancer Res. Clin. Oncol. **129:**621–630.
2. **Bashir, T., N. V. Dorrello, V. Amador, D. Guardavaccaro, and M. Pagano.** 2004. Control of the SCF(Skp2-Cks1) ubiquitin ligase by the APC/C(Cdh1) ubiquitin ligase. Nature **428:**190–193.
3. **Bharadwaj, R., and H. Yu.** 2004. The spindle checkpoint, aneuploidy, and cancer. Oncogene **23:**2016–2027.
4. **Brown, K. D., R. M. Coulson, T. J. Yen, and D. W. Cleveland.** 1994. Cyclin-like accumulation and loss of the putative kinetochore motor CENP-E results from coupling continuous synthesis with specific degradation at the end of mitosis. J. Cell Biol. **125:**1303–1312.
5. **Bu, W., and L. K. Su.** 2001. Regulation of microtubule assembly by human EB1 family proteins. Oncogene **20:**3185–3192.
6. **Burton, J. L., and M. J. Solomon.** 2001. D box and KEN box motifs in budding yeast Hsl1p are required for APC-mediated degradation and direct binding to Cdc20p and Cdh1p. Genes Dev. **15:**2381–2395.
7. **Castro, A., S. Vigneron, C. Bernis, J. C. Labbe, and T. Lorca.** 2003. Xkid is degraded in a D-box, KEN-box, and A-box-independent pathway. Mol. Cell. Biol. **23:**4126–4138.
8. **Clute, P., and J. Pines.** 1999. Temporal and spatial control of cyclin B1 destruction in metaphase. Nat. Cell Biol. **1:**82–87.
9. **Donzelli, M., M. Squatrito, D. Ganoth, A. Hershko, M. Pagano, and G. F. Draetta.** 2002. Dual mode of degradation of Cdc25 A phosphatase. EMBO J. **21:**4875–4884.
10. **Doxsey, S., W. Zimmerman, and K. Mikule.** 2005. Centrosome control of the cell cycle. Trends Cell Biol. **15:**303–311.
11. **Eichmuller, S., D. Usener, R. Dummer, A. Stein, D. Thiel, and D. Schadendorf.** 2001. Serological detection of cutaneous T-cell lymphoma-associated antigens. Proc. Natl. Acad. Sci. USA **98:**629–634.
12. **Fang, G., H. Yu, and M. W. Kirschner.** 1998. Direct binding of CDC20 protein family members activates the anaphase-promoting complex in mitosis and G1. Mol. Cell **2:**163–171.
13. **Gadde, S., and R. Heald.** 2004. Mechanisms and molecules of the mitotic spindle. Curr. Biol. **14:**R797–R805.
14. **Ganem, N. J., and D. A. Compton.** 2004. The KinI kinesin Kif2a is required for bipolar spindle assembly through a functional relationship with MCAK. J. Cell Biol. **166:**473–478.
15. **Gordon, D. M., and D. M. Roof.** 2001. Degradation of the kinesin Kip1p at anaphase onset is mediated by the anaphase-promoting complex and Cdc20p. Proc. Natl. Acad. Sci. USA **98:**12515–12520.
16. **Goshima, G., and R. D. Vale.** 2003. The roles of microtubule-based motor proteins in mitosis: comprehensive RNAi analysis in the *Drosophila* S2 cell line. J. Cell Biol. **162:**1003–1016.
17. **Harper, J. W., J. L. Burton, and M. J. Solomon.** 2002. The anaphase-promoting complex: it's not just for mitosis any more. Genes Dev. **16:**2179–2206.
18. **Hildebrandt, E. R., and M. A. Hoyt.** 2001. Cell cycle-dependent degradation of the *Saccharomyces cerevisiae* spindle motor Cin8p requires APC(Cdh1) and a bipartite destruction sequence. Mol. Biol. Cell **12:**3402–3416.
19. **Horesh, D., T. Sapir, F. Francis, S. G. Wolf, M. Caspi, M. Elbaum, J. Chelly, and O. Reiner.** 1999. Doublecortin, a stabilizer of microtubules. Hum. Mol. Genet. **8:**1599–1610.
20. **Inoue, Y. H., M. do Carmo Avides, M. Shiraki, P. Deak, M. Yamaguchi, Y. Nishimoto, A. Matsukage, and D. M. Glover.** 2000. Orbit, a novel microtubule-associated protein essential for mitosis in *Drosophila melanogaster*. J. Cell Biol. **149:**153–166.
21. **Iyer, V. R., M. B. Eisen, D. T. Ross, G. Schuler, T. Moore, J. C. Lee, J. M. Trent, L. M. Staudt, J. Hudson, Jr., M. S. Boguski, D. Lashkari, D. Shalon, D. Botstein, and P. O. Brown.** 1999. The transcriptional program in the response of human fibroblasts to serum. Science **283:**83–87.
22. **Jeon, S. M., B. Choi, K. U. Hong, E. Kim, Y. S. Seong, C. D. Bae, and J. Park.** 2006. A cytoskeleton-associated protein, TMAP/CKAP2, is involved in the proliferation of human foreskin fibroblasts. Biochem. Biophys. Res. Commun. **348:**222–228.
23. **Jin, Y., Y. Murakumo, K. Ueno, M. Hashimoto, T. Watanabe, Y. Shimoyama, M. Ichihara, and M. Takahashi.** 2004. Identification of a mouse cytoskeleton-associated protein, CKAP2, with microtubule-stabilizing properties. Cancer Sci. **95:**815–821.
24. **Juang, Y. L., J. Huang, J. M. Peters, M. E. McLaughlin, C. Y. Tai, and D. Pellman.** 1997. APC-mediated proteolysis of Ase1 and the morphogenesis of the mitotic spindle. Science **275:**1311–1314.
25. **Kapoor, T. M., T. U. Mayer, M. L. Coughlin, and T. J. Mitchison.** 2000. Probing spindle assembly mechanisms with monastrol, a small molecule inhibitor of the mitotic kinesin, Eg5. J. Cell Biol. **150:**975–988.
26. **Ke, P. Y., and Z. F. Chang.** 2004. Mitotic degradation of human thymidine kinase 1 is dependent on the anaphase-promoting complex/cyclosome-CDH1-mediated pathway. Mol. Cell. Biol. **24:**514–526.
27. **Kline-Smith, S. L., and C. E. Walczak.** 2004. Mitotic spindle assembly and chromosome segregation: refocusing on microtubule dynamics. Mol. Cell **15:**317–327.
28. **Lindon, C., and J. Pines.** 2004. Ordered proteolysis in anaphase inactivates Plk1 to contribute to proper mitotic exit in human cells. J. Cell Biol. **164:**233–241.
29. **Maiato, H., E. A. Fairley, C. L. Rieder, J. R. Swedlow, C. E. Sunkel, and W. C. Earnshaw.** 2003. Human CLASP1 is an outer kinetochore component that regulates spindle microtubule dynamics. Cell **113:**891–904.
30. **Maouche-Chretien, L., N. Deleu, C. Badoual, P. Fraissignes, R. Berger, P.**

Gaulard, P. H. Romeo, and K. Leroy-Viard. 1998. Identification of a novel cDNA, encoding a cytoskeletal associated protein, differentially expressed in diffuse large B cell lymphomas. Oncogene **17:**1245–1251.
31. **Meng, L., R. Mohan, B. H. Kwok, M. Elofsson, N. Sin, and C. M. Crews.** 1999. Epoxomicin, a potent and selective proteasome inhibitor, exhibits in vivo anti-inflammatory activity. Proc. Natl. Acad. Sci. USA **96:**10403–10408.
32. **Nguyen, H. G., D. Chinnappan, T. Urano, and K. Ravid.** 2005. Mechanism of Aurora-B degradation and its dependency on intact KEN and A-boxes: identification of an aneuploidy-promoting property. Mol. Cell. Biol. **25:** 4977–4992.
33. **Nigg, E. A.** 2002. Centrosome aberrations: cause or consequence of cancer progression? Nat. Rev. Cancer. **2:**815–825.
34. **Paoletti, A., M. Moudjou, M. Paintrand, J. L. Salisbury, and M. Bornens.** 1996. Most of centrin in animal cells is not centrosome-associated and centrosomal centrin is confined to the distal lumen of centrioles. J. Cell Sci. **109:**3089–3102.
35. **Pfleger, C. M., and M. W. Kirschner.** 2000. The KEN box: an APC recognition signal distinct from the D box targeted by Cdh1. Genes Dev. **14:**655–665.
36. **Pfleger, C. M., E. Lee, and M. W. Kirschner.** 2001. Substrate recognition by the Cdc20 and Cdh1 components of the anaphase-promoting complex. Genes Dev. **15:**2396–2407.
37. **Pierre, P., R. Pepperkok, and T. E. Kreis.** 1994. Molecular characterization of two functional domains of CLIP-170 in vivo. J. Cell Sci. **107:**1909–1920.
38. **Raemaekers, T., K. Ribbeck, J. Beaudouin, W. Annaert, M. Van Camp, I. Stockmans, N. Smets, R. Bouillon, J. Ellenberg, and G. Carmeliet.** 2003. NuSAP, a novel microtubule-associated protein involved in mitotic spindle organization. J. Cell Biol. **162:**1017–1029.
39. **Salic, A., J. C. Waters, and T. J. Mitchison.** 2004. Vertebrate shugoshin links sister centromere cohesion and kinetochore microtubule stability in mitosis. Cell **118:**567–578.
40. **Schwab, M., A. S. Lutum, and W. Seufert.** 1997. Yeast Hct1 is a regulator of Clb2 cyclin proteolysis. Cell **90:**683–693.
41. **Stewart, S., and G. Fang.** 2005. Destruction box-dependent degradation of aurora B is mediated by the anaphase-promoting complex/cyclosome and Cdh1. Cancer Res. **65:**8730–8735.
42. **Tinker-Kulberg, R. L., and D. O. Morgan.** 1999. Pds1 and Esp1 control both anaphase and mitotic exit in normal cells and after DNA damage. Genes Dev. **13:**1936–1949.
43. **Tsuchihara, K., V. Lapin, C. Bakal, H. Okada, L. Brown, M. Hirota-Tsuchihara, K. Zaugg, A. Ho, A. Itie-Youten, M. Harris-Brandts, R. Rottapel, C. D. Richardson, S. Benchimol, and T. W. Mak.** 2005. Ckap2 regulates aneuploidy, cell cycling, and cell death in a p53-dependent manner. Cancer Res. **65:**6685–6691.
44. **Visintin, R., S. Prinz, and A. Amon.** 1997. CDC20 and CDH1: a family of substrate-specific activators of APC-dependent proteolysis. Science **278:**460–463.
45. **Weisshaar, B., T. Doll, and A. Matus.** 1992. Reorganisation of the microtubular cytoskeleton by embryonic microtubule-associated protein 2 (MAP2c). Development **116:**1151–1161.
46. **Weissman, A. M.** 2001. Themes and variations on ubiquitylation. Nat. Rev. Mol. Cell. Biol. **2:**169–178.
47. **Whitfield, M. L., G. Sherlock, A. J. Saldanha, J. I. Murray, C. A. Ball, K. E. Alexander, J. C. Matese, C. M. Perou, M. M. Hurt, P. O. Brown, and D. Botstein.** 2002. Identification of genes periodically expressed in the human cell cycle and their expression in tumors. Mol. Biol. Cell **13:**1977–2000.
48. **Zhu, C., J. Zhao, M. Bibikova, J. D. Leverson, E. Bossy-Wetzel, J. B. Fan, R. T. Abraham, and W. Jiang.** 2005. Functional analysis of human microtubule-based motor proteins, the kinesins and dyneins, in mitosis/cytokinesis using RNA interference. Mol. Biol. Cell **16:**3187–3199.
49. **Zou, H., T. J. McGarry, T. Bernal, and M. W. Kirschner.** 1999. Identification of a vertebrate sister-chromatid separation inhibitor involved in transformation and tumorigenesis. Science **285:**418–422.
50. **Zur, A., and M. Brandeis.** 2002. Timing of APC/C substrate degradation is determined by fzy/fzr specificity of destruction boxes. EMBO J. **21:**4500–4510.